DYNAMICS SENSITIVITY STUDY OF STOCK CAR SHIFTER COMPONENTS

by

Samuel Cole DesRocher

A thesis submitted to the faculty of
The University of North Carolina at Charlotte
in partial fulfillment of the requirements
for the degree of Master of Science in
Mechanical Engineering

Charlotte

2016

Approved by:

_____
Dr. Tony Schmitz

_____
Dr. Matthew Davies

_____
Dr. John Ziegert

ABSTRACT

SAMUEL COLE DESROCHER. Dynamics sensitivity study of stock car shifter components (Under the direction of DR. TONY SCHMITZ)

Previous experience in race situations has shown that components in the shifter section of the stock car drivetrain are subject to failure. As the engine operates in a specific rotational speed band throughout a race event due to gearing rules, the drivetrain components may experience vibrations imposed by that frequency band. It was desired to determine the influence of exchanging components – namely the setback brackets and shifter handle – within the shifter assembly. In preparation for potential design changes, an experimental study was performed using a simplified setup. The outcome of this study is the topic of this thesis.

In the simplified setup, only the setback brackets, shifter tower, and shifter handle were included. These were attached to a rigid mass, rather than the stock car drivetrain. Both Finite Element Analysis (FEA) and modal analysis were used to study this simplified model. Modal testing was performed on both the simplified model and the stock car to understand the model limitations. Analysis of these two test set-ups revealed that the simplified model did not fully represent the real system. The natural frequencies of the three modes found in the simplified model matched the stock car measurements to within 17%. However, additional modes were found that were specific only to the car.

Based on these results, it is recommended that the simplified FEA model should be further developed to include all modes obtained from the stock car modal analysis test results. Once a reasonable comparison is achieved, the sensitivity design study may be completed.

ACKNOWLEDGEMENTS

This work would not be possible without the assistance of Hendrick Motorsports providing the topic for this project as well as the CAD and FEA systems. Multiple employees also deserve acknowledgement for their assistance in constructing the modal testing setup.

In addition to being Chair of the Advisory Committee, Dr. Tony Schmitz has contributed to this research though the use of modal analysis equipment and evaluation software. Appreciation also goes out to Dr. Matthew Davies and Dr. John Ziegert for their roles as members of the Advisory Committee.

TABLE OF CONTENTS

LIST OF TABLES

LIST OF FIGURES

LIST OF ABBREVIATIONS

ADC	analog-to-digital converter
DFT	discrete Fourier transform
FEA	finite element analysis
FEM	finite element model file, NX/Nastran
FRF	frequency response function
NASCAR	National Association for Stock Car Auto Racing
SIM	simulation file, NX/Nastran

CHAPTER 1: INTRODUCTION

Within the definition of the rules of the NASCAR Sprint Cup Series, design changes for the transmission, shifter, and other drivetrain components is largely guided by vendors and, even so, these changes are restricted for cost purposes. Therefore, most components are subject to vibrations created from engine and transmission imbalances.

The goal of this thesis is to first determine the correlation between a simplified model of the shifter handle assembly and then evaluate a matrix of setback brackets and shifter handle designs to determine which, if any, of the components can shift the natural frequencies of the system sufficiently to reduce vibration amplitudes. To be more specific, the system is to be more closely examined for the response at the shifter to determine if a distinction can be made as to which combination of components can shift the natural frequency out of the band of the engine frequency or its multiples.

The modal response of the system will be evaluated in two manners: 1) through finite element analysis (FEA); and 2) through modal analysis using an impact hammer and accelerometer.

CHAPTER 2: MATERIALS AND METHODS

2.1 Modal Testing Background

Modal testing is an experimental means of obtaining the dynamic characteristics of either a single object or of an assembly. A basic overview of the process is provided here:

1. Exciting the object/assembly
2. Measuring the vibration response
3. Transferring the measurement into usable and readable data
4. Analyzing the data to determine the dynamic response characteristics.

Each of these steps has various options; some are more suited to certain situations than others.

For the first step, the most common excitation mechanisms are shakers and impact hammers. The former allows for inputs that are periodic, such as a sine wave, as well as random. The latter is used to apply an impulse force; due to the short time duration of this test, multiple samples are often completed and averaged in the frequency domain. In either case, the excitation must encompass the desired frequency range for the structure to be analyzed (Schmitz & Smith, 2012).

The second, or measurement, step is split between two transducer types: contact and non-contact. The contact transducers are accelerometers that are mounted on the structure during the testing phase. These typically use an internal piezoelectric crystal that gets squeezed by a seismic mass under acceleration to produce a charge, which is amplified to produce a voltage. Non-contact transducers include capacitance probes and laser vibrometers. Capacitance probes are dependent on the voltage of two charged bodies (one being the probe) and the dielectric constant of the material between them. As the distance between the bodies grows, the capacitance changes proportionally. Laser vibrometers operate by using the Doppler shift of the laser beam's frequency to detect the speed at which the target object is vibrating. The non-contact options are the preferred method as they do not add mass to the system under study. This becomes more important as the mass of the accelerometer approaches the modal mass of the system. However, it is often easier and less expensive to set up the accelerometers, especially in a more mobile environment. (Schmitz & Smith, 2012)

A dynamic signal analyzer, used in the third step, is able to take time-domain signal inputs from the force input mechanism and the transducer and calculate the Fourier transform of each. The input signals are sent through amplifiers and analog-to-digital converters (ADC) before entering the signal analyzer. Often, the analyzers include an internal anti-aliasing filter that the signal encounters before calculating the discrete Fourier transform (DFT). The analyzer then calculates the ratio of the frequency domain vibration to the force. This is the output FRF as displayed in FIGURE 1. Depending on the transducer, the outputs can include displacement, velocity, or acceleration of the

system under observation. Therefore, the ratio given as an output by the analyzer may take one of the three forms listed in TABLE 1.

The receptance type yields a FRF composed of the Fourier transform of both the input force, F(ω), and the resulting response signal, X(ω):

$$H(\omega) = \frac{X(\omega)}{F(\omega)} \quad (1).$$

TABLE 1 : FRF types

FRF type	**Transducer type**
Receptance/compliance	Displacement
Mobility	Velocity
Accelerance/inertance	Acceleration

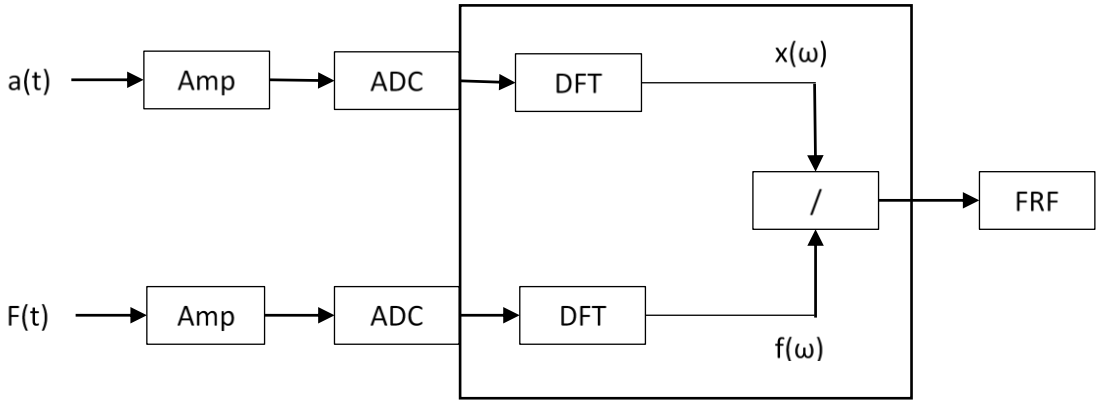

FIGURE 1 : Flow diagram for a typical dynamic signal analyzer

2.2 NASCAR Vehicle Background

2.2.1 NASCAR Drivetrain

For cost reasons, the sanctioning body has restrictions on many areas of the car. This allows a greater number of participants to be more competitive as they are not at such great disadvantages when it comes to funding. This prevents more exotic materials and geometries from being introduced for efficiencies, aerodynamic gain, and lighter weight because these may be more difficult to inspect, decrease competition, and potentially lead to injuries upon failure. Among the list of mandated components are driveshaft materials and geometries as well as rear gear ratios. In some areas of the vehicle, competitors are reliant upon the pre-approval of vendor components in order to begin use.

These mandates can vary between circuits and even between return trips to a given circuit within a calendar year. This makes designing shifter components to have natural frequencies in a certain bandwidth difficult. Thus, determining whether combinations of existing components may be preferred at certain tracks where the engine and driveline speeds spend larger amounts of time at a certain frequency is a difficult task. Since the shifter components have had a tendency to break on occasion through the years and these failures are difficult to replicate in physical testing, it was decided to begin the evaluation with components in the shifter sub-assembly.

2.2.2 Car Coordinate System

This section describes the right-handed coordinate system used in the analysis. The positive x-axis points toward the rear of the vehicle. Next, the positive y-axis is directed toward the "passenger" side of the chassis. Following the right-hand-rule, the positive z-direction points upward through the roof. The vehicle origin is located on the bottom of the truck arm cross-member on the centerline of the car. The coordinate system is shown in relation to the car body in FIGURE 2.

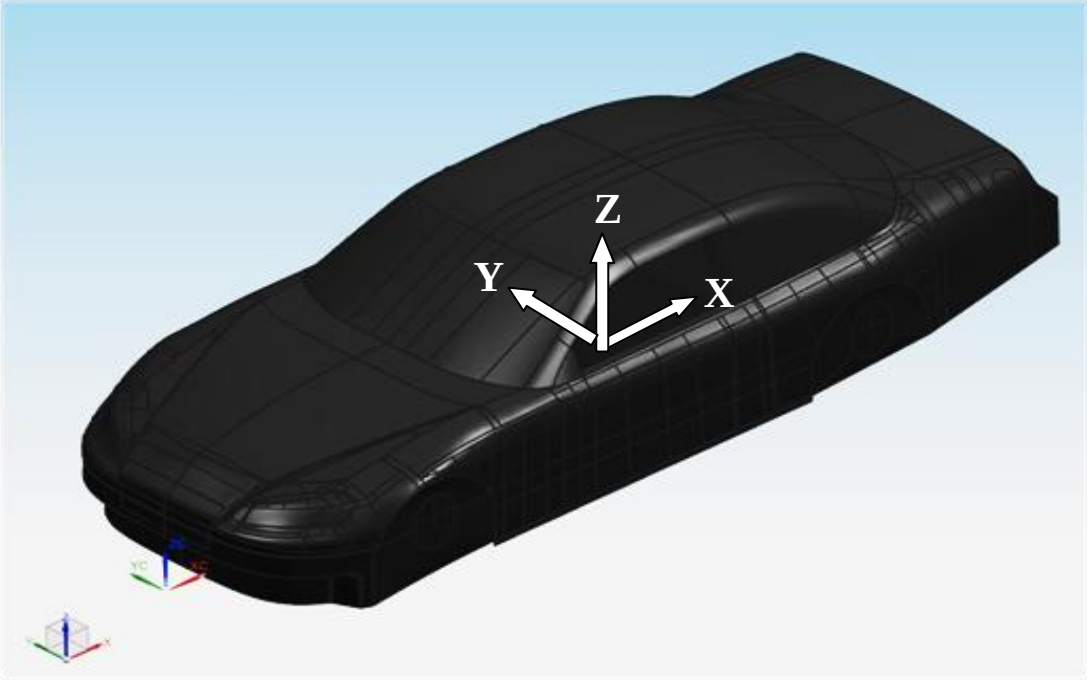

FIGURE 2 : Coordinate system in relation to the car body

2.2.3 Simplified Shifter Model

The nature and size of the vehicle drivetrain does not lend itself easily to an all-inclusive vibration analysis. To minimize the finite element computational requirements, a simplified model of the system was proposed and constructed to evaluate as an alternative. The simplified model includes the following as the main components in the assembly: setback brackets, shifter tower, and shifter handle. The assembly is displayed in FIGURE 3.

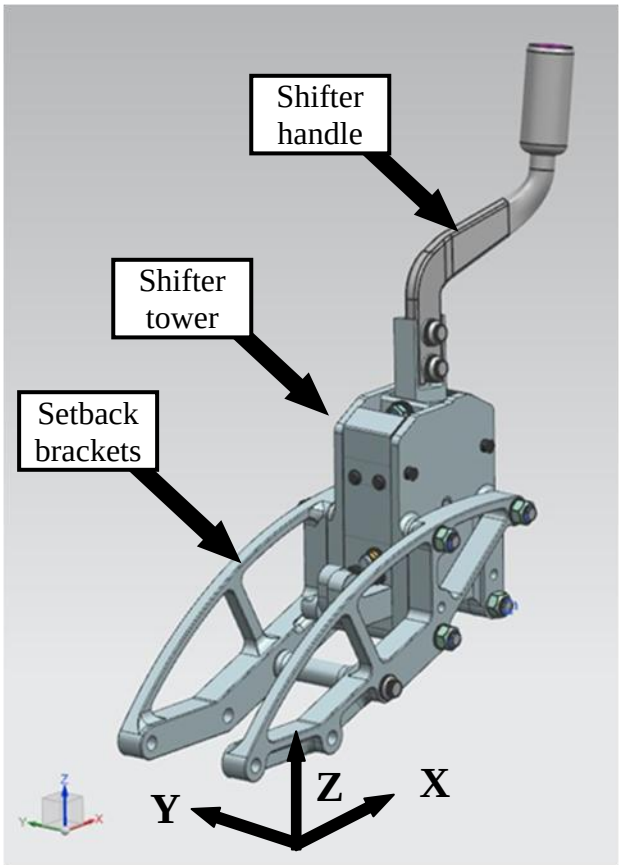

FIGURE 3 : Simplified model including setback brackets, shifter tower, and shifter handle

This model is based on the assumption that the rest of the drivetrain, especially the tail housing to which the setback brackets are normally bolted, are infinitely stiff and insignificant in contribution to the vibration of the shifter handle. Potential issues with this assumption begin with the infinite stiffness and mass of the tail housing, which are not correct. Furthermore, the tail housing is constrained on either end to the main housing and the driveshaft universal joint yoke.

2.3 Modal Testing Analysis Setup

The car setup is not conducive to shaker excitation. Therefore, excitation options such as stepped-sine, slow sine sweep, linear sweep, logarithmic sweep, other periodic excitation, and random excitation are more difficult to implement (Ewins, 1995). Even the transient inputs, such as chirp (also known as rapid sine sweep) and burst (a short section of a periodic or random signal), are not plausible options since they also require a shaker. This leaves the impact hammer excitation as a viable method for force input into the system. There is also convenience in this method as the equipment is accessible.

This method is conducted by repeating the hammer impacts under the same conditions in order to average the FRF results. A larger sample size will decrease random noise effects; thus, a tradeoff arises between response accuracy and measurement time (Ewins, 1995).

The use of impact testing has negative aspects as well. Since the impact hammer generally requires human input, additional error is introduced into the system. Ideally, the force input and the measurement instruments are aligned in the same direction. Unfortunately, adding a human component to the system increases the likelihood of this not happening. It also adds a degree of uncertainty to the consistency if performing multiple measurements. Furthermore, for this method to be performed correctly, the entire response must be recorded from the moment of hammer impact until the response has died out. This is because impact hammers excite multiple frequencies at the same time (Ewins, 1995). This requirement will not be difficult to reach in this instance as the system has significant damping leading to a short response time.

Regarding the dynamic signal analyzer, MetalMAX^{TM} software is capable of taking the inputs from the impact hammer and the accelerometer (serial and model numbers included in Appendix I). As additional measurements are performed, the software is capable of auto-averaging each of the trials. In addition, the software can also allow the user to observe the measurement coherence to evaluate the reliability.

2.4 FEA Evaluation

As an alternative to physical testing, numerical analysis is also available through FEA modeling. While the initial thought may be that this method is easier, the realistic view is that the results are only as good as the model under evaluation. Therefore, specifics such as material assignment, accurate geometry representation (including joint interfaces), boundary condition definition, and damping are crucial in defining the model.

In order to complement the physical evaluation, the matrix of assembly options was also evaluated using NX Nastran FEA software. The Advanced Simulation module allows for an evaluation of modal frequencies, both bending and torsional. While the software does allow for damping through different constraints, internal damping is not available for any material meshes.

Pinned constraints were placed in each of the setback brackets where they are normally bolted to the top of the tail housing. In other positions, surface-to-surface glue constraints were used in the SIM file to connect the individual component meshes created in the FEM file. These constraints are displayed in FIGURE 4. The simplified model may be likened to a cantilever where the pin constraints affix the cantilever base to the ground.

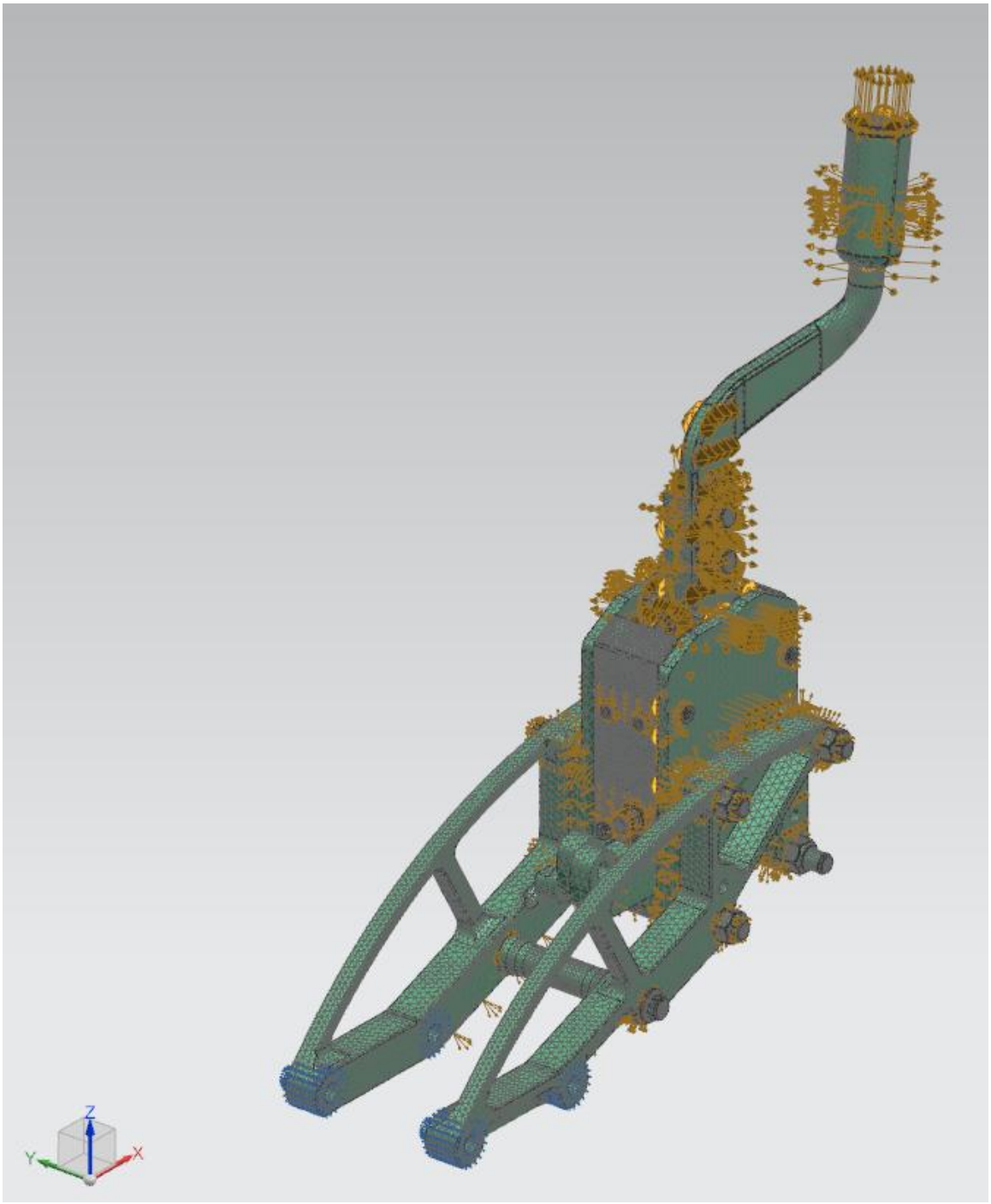

FIGURE 4 : FEM file displaying pinned boundary constraints (blue) and glued inter-mesh constraints (yellow)

2.5 Connection from FEA to in-car Operation

Due to the complexity of the stock car and associated model, the simplified model was evaluated as an intermediate solution. Both FEA and modal testing were used to evaluate the simplified model.

In order to confirm the efficacy of the simplified model, existing race-used components were initially included in the simplified FEA model. In addition, the physical realization of this model used an aluminum block with an approximate weight of 48 lbf. It is displayed in FIGURE 5, and the engineering drawing is included in Appendix II. This block represents the large mass of the rest of the drivetrain, specifically the tail housing. The physical representation of the simplified model made use of 26” setback brackets as well as a shifter handle constructed of 7075 aluminum.

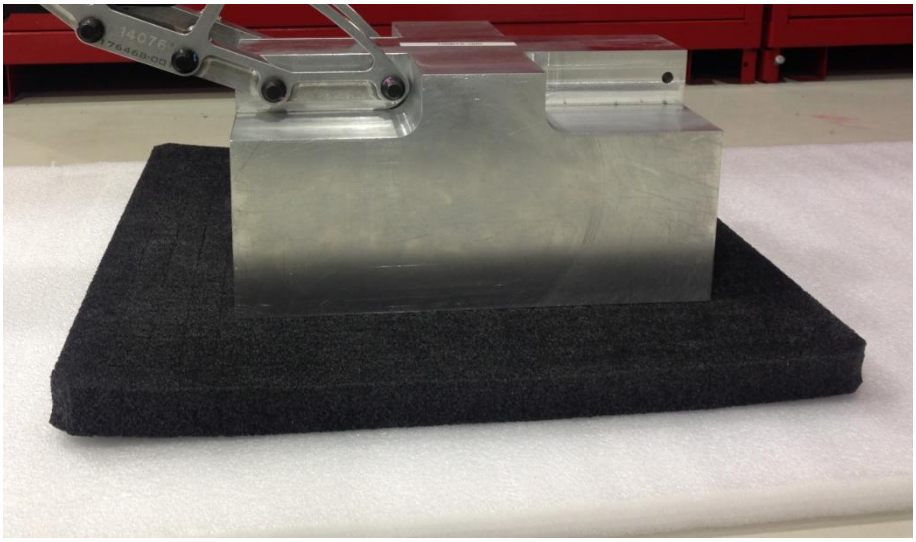

FIGURE 5 : Aluminum block for physical realization of simplified model

Two comparisons were performed. First, the FEA and modal testing results for the simplified model were compared. This enabled the accuracy of the FEA to be evaluated. Second, measurements on a stock car shifter assembly were compared to the simplified model to determine the usefulness of the physical model (i.e., determine if it adequately represents the actual stock car). This process is depicted in FIGURE 6.

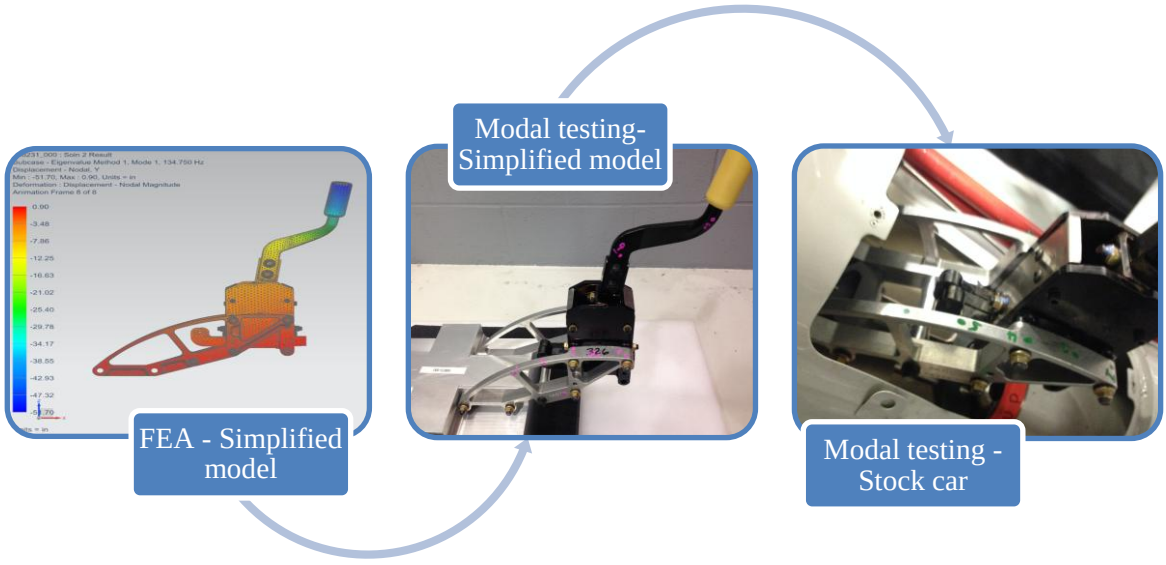

FIGURE 6 : Illustration of the link between computer model and actual assembly

CHAPTER 3: RESULTS

3.1 Comparison of FEA and Real World Simplified Models

The simplified model FEA and modal testing results are compared in this section. The natural frequencies obtained from FEA are listed according to direction of vibration in TABLE 2. The modes are denoted with an "F" to represent the FEA model result. The first mode occurs primarily in only one of the Cartesian directions, while the second and third modes occur in a combination of axes.

Figures 7-10 show the three modes listed in TABLE 2. In the images from the FEA, the legend is based upon a nominal force input resulting in a displacement value. For mode shape evaluation, the value of the legend may be ignored with attention being paid to the relative color intensity. (Additional images displaying these modes may be found in Appendix III).

TABLE 2 : Natural frequency results of simplified model FEA

Mode	Frequency (Hz)		
	X	Y	Z
1F		134.8	
2F	148.4		148.4
3F	225.4	225.4	225.4

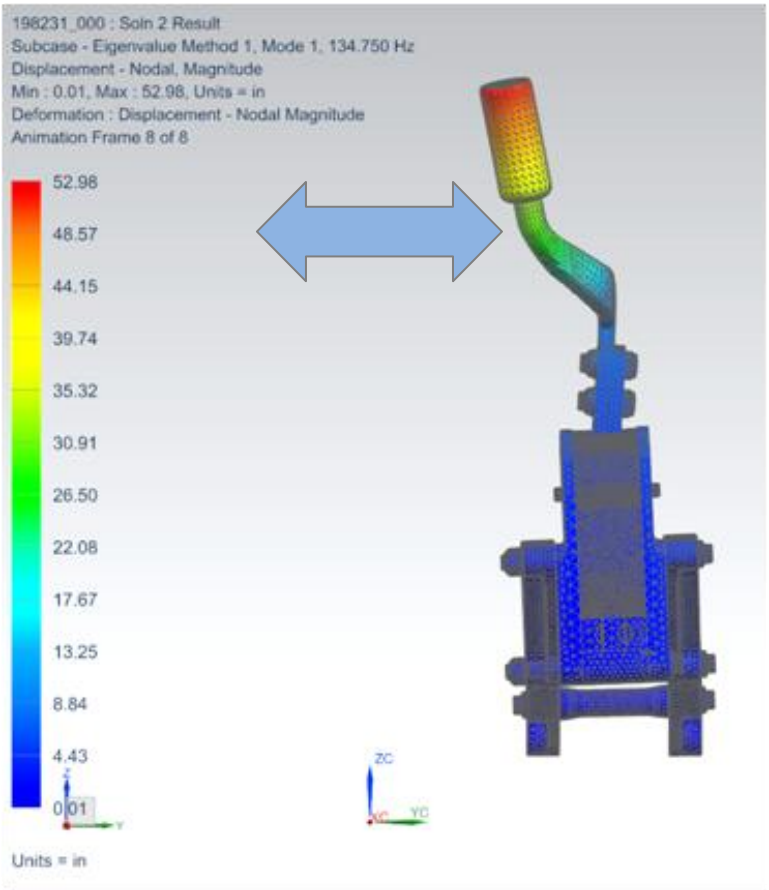

FIGURE 7 : Mode 1F looking at the yz plane from the +x direction

Mode 1F is bending of the shifter handle, the section above the main tower, in the y-direction. This mode is displayed in FIGURE 7. In this mode, the rest of the assembly exhibits motion which is orders of magnitude less than the handle. The handle is acting as a cantilever attached to the shifter tower. As the cross section of the cantilevered handle is thinnest in this direction, it is expected to bend in this direction with the largest amplitude and lowest natural frequency.

Mode 2F is a vertical shaking of the entire system mainly as a result of the upper section flexibility of the setback brackets. This thinner section is shown in a stretched and displaced manner. In this mode, the setback brackets are acting as a

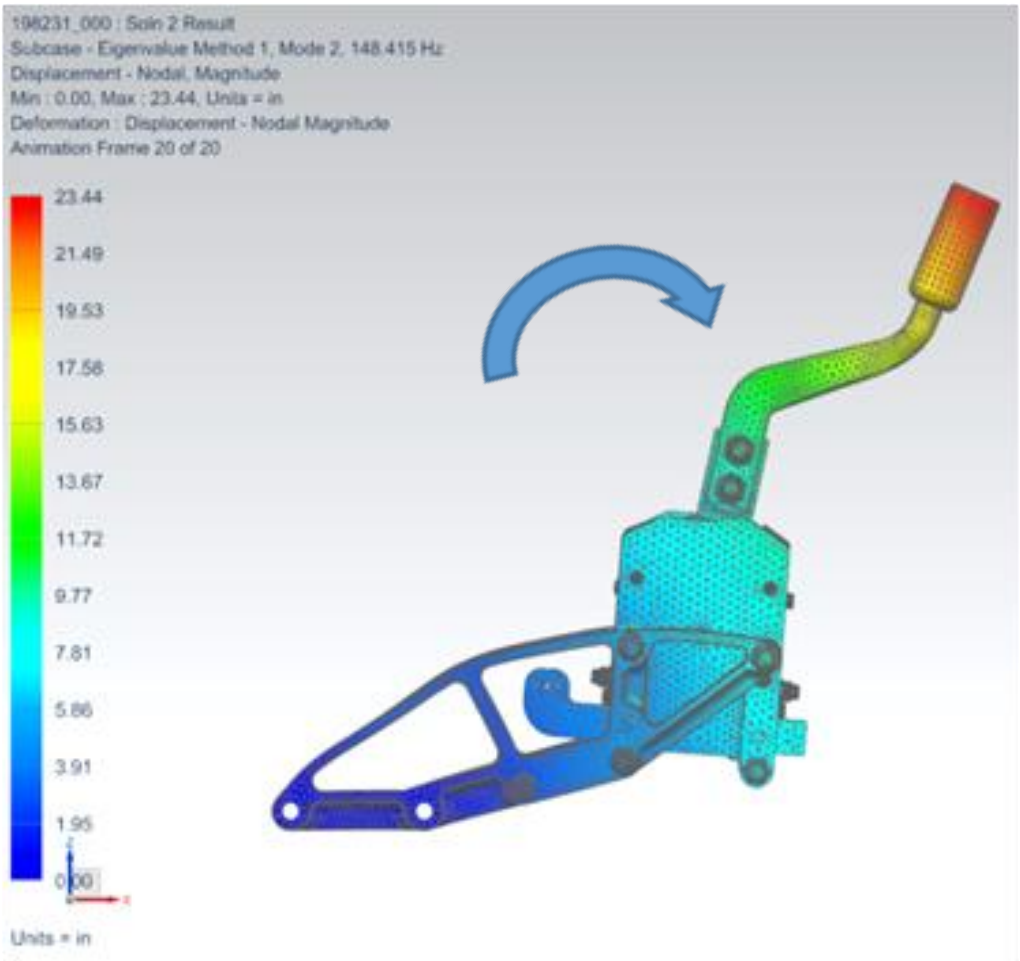

FIGURE 8 : Mode 2F looking at the xz-plane from the –y direction

cantilever off of the tail housing which is represented in the FEA model by the pinned constraints. The vertical z-axis motion of the system is also relayed into a fore-aft vibration in the x-direction that is most evident at the tip of the handle. This motion is displayed in FIGURE 8. Though the displacement is much lower than the other axes, a slight y-axis contribution may be seen by a minor rotation as observed from the rear in FIGURE 9.

Mode 3F is similar to the second bending mode of a cantilever, having one node at the fixed end as well as one at a point between the ends. In this instance, the setback brackets

are bending and twisting in one direction while the handle itself is out of phase with that motion. This phase difference is displayed in FIGURE 10. The setback brackets are twisting about a line parallel to the x-axis but are moving vertically. The handle is again moving in the y-direction similar to the first mode. The node is located near the center of the shifter tower. The only movement in the x-direction is a result of the tip of the handle pivoting around where it is bolted to the shifter tower.

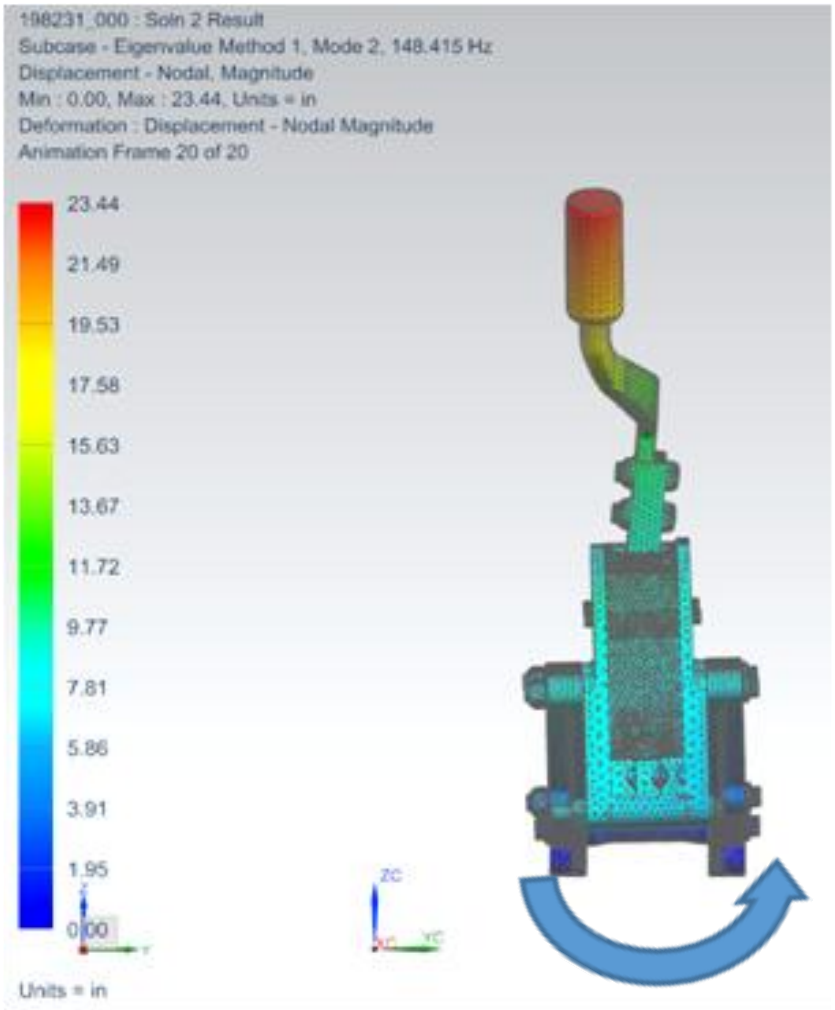

FIGURE 9 : Mode 2F looking at the yz-plane from the –x direction

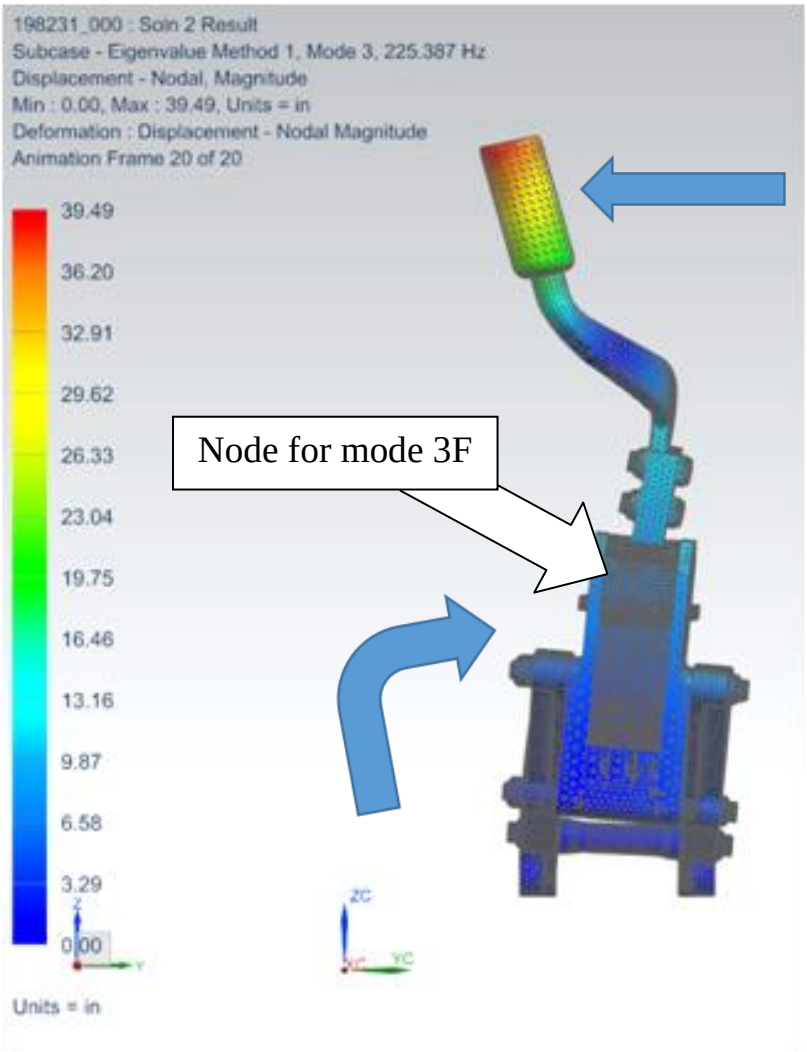

FIGURE 10 : Mode 3F from simplified model FEA looking at the yz-plane from the +x direction

For the modal analysis, nine total points were selected in regard to accessibility in the car to aid in the second comparison between the block and stock car. These test points are illustrated in Figures 11 and 12. Additional images are found in Appendix IV.

The modal analysis test on the simplified model block yielded similar results to the FEA. One difference was the presence of four modes under 50 Hz that were not output from the FEA. These could be a result of the nominally “free” boundary constraint

imposed by resting the entire assembly on soft foam. The modes listed in TABLE 3 are those that are above the 50 Hz limit. These modes are denoted by a “B” to denote the physical simplified model with the aluminum block. The natural frequencies in each the X, Y, and Z directions have been labeled and organized as similar frequencies. This sorting provides for aligning possible rotational mode shapes that would be captured in multiple directions. Meanwhile the three modes obtained above 50 Hz were similar in natural frequency and mode shapes to those found in the FEA.

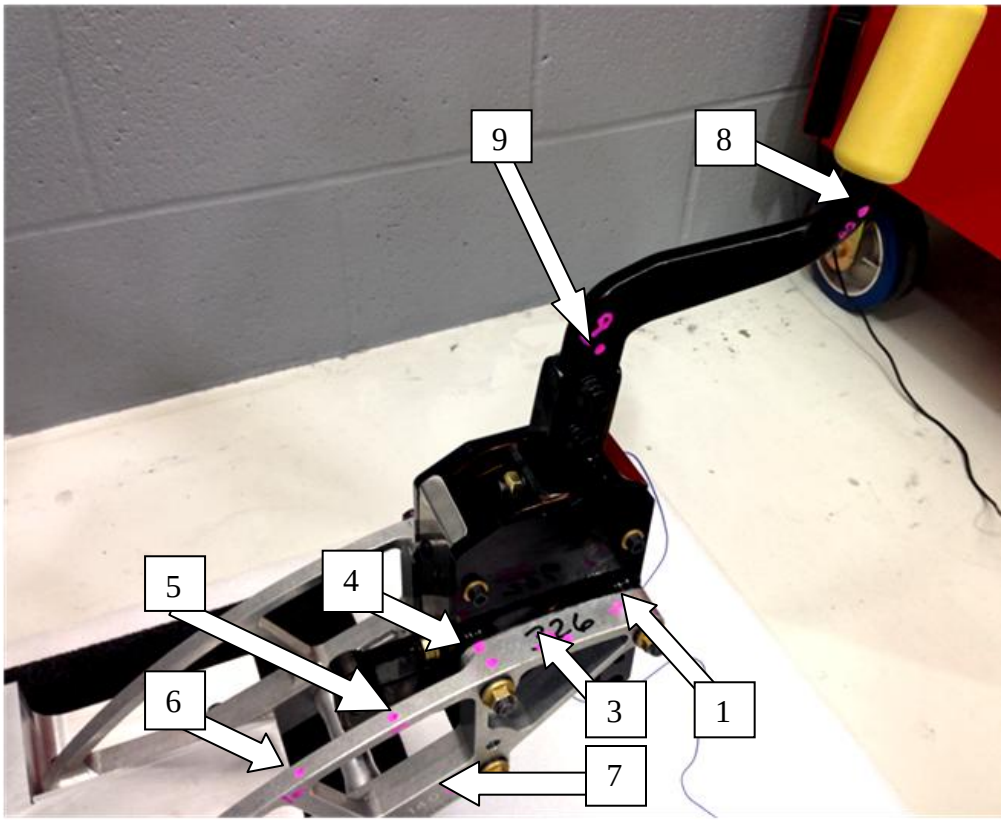

FIGURE 11 : Isometric view of simplified model modal analysis test with location points

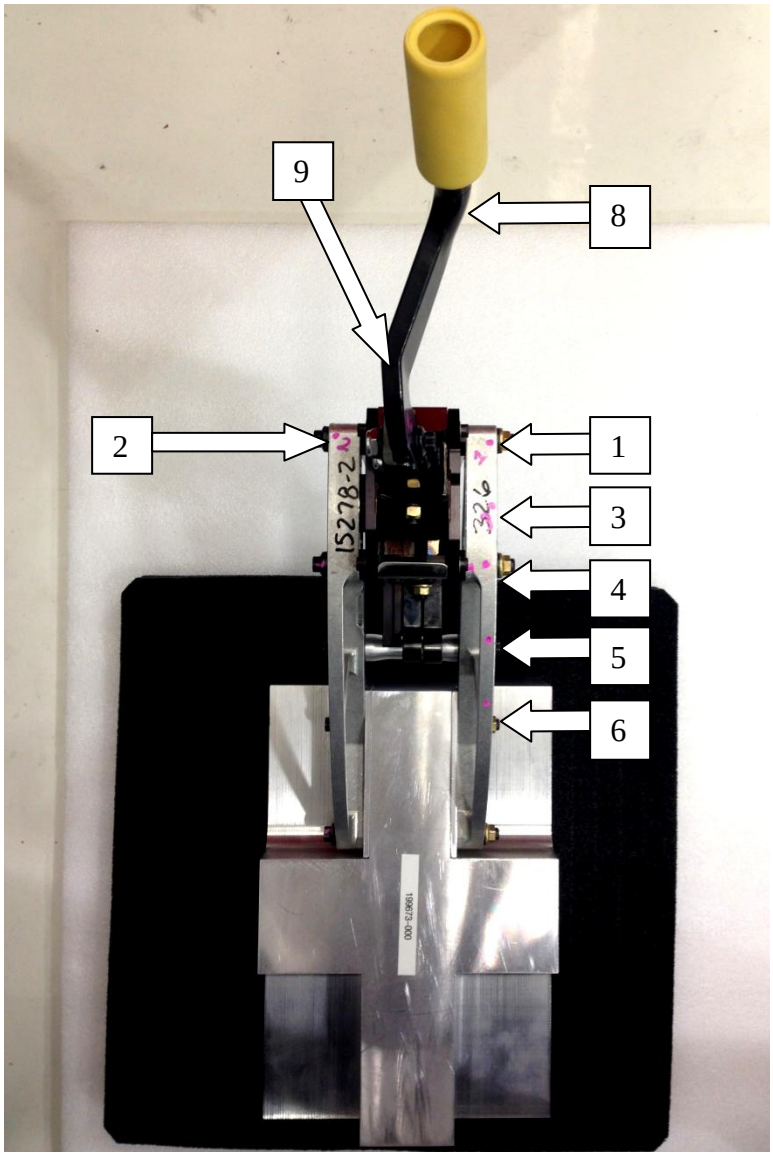

FIGURE 12 : Top view of simplified model modal analysis test with location points

TABLE 3 : Natural frequencies determined from modal analysis of simplified model

Mode	Frequency (Hz)		
	X	Y	Z
1B	-	141.5	-
2B	146.5	146.5	146.1
3B	269.8	273.1	272.8

Mode 1B from the modal testing in TABLE 3 was similar to that shown from the FEA in that it represented the shifter handle oscillating in the y-direction. The difference here is that it occurs at 141.5 Hz from the modal testing and at 134.8 Hz from the computer model.

Mode 2B is comparable to mode 2F and has a closer natural frequency. The computer simulation output a natural frequency of 148.4 Hz, where the measurements yielded an average result of 147.1 Hz from all three coordinate axes.

Mode 3B occurs at 271.9 Hz based on the physical analysis. The computer model places this mode at 225.4 Hz. While there is a discrepancy in the natural frequency, the mode shapes between the physical and computational models are similar. Again, this mode is likened to the second bending mode of a fixed-free beam. The main bending occurs in the setback brackets, and the handle is out of phase with the bending of the setback brackets.

The frequencies determined between the two methods are compared in TABLE 4, with the frequencies aligned via similar mode shapes. The first two modes are within 5.0% between the physical and simulated models. As noted in the above description, the third mode has a natural frequency discrepancy greater than 20.0% between the two models.

TABLE 4 : Comparison of similar modes from FEA and modal analysis for the simplified model

FEA		Modal Analysis		% Difference
Mode	**Frequency (Hz)**	**Mode**	**Frequency (Hz)**	
1F	134.8	**1B**	141.5	5.0%
2F	148.4	**2B**	146.4	-1.4%
3F	225.4	**3B**	271.9	20.6%

For the cantilever shape for modes 1B and 1F, the primary motion is the handle oscillating in the y-direction. Normalized mode shapes taken from both the FEA results and modal analysis for the simplified model are shown in FIGURE 13.

Mode 2 (B and F) represents a primarily vertical bending of the system rotating about the mounting position to the tail housing. The normalized mode shapes are compared in FIGURE 14. Since the vertical rotation becomes transferred into the x-direction, the mode shapes are also given for this axis in FIGURE 15.

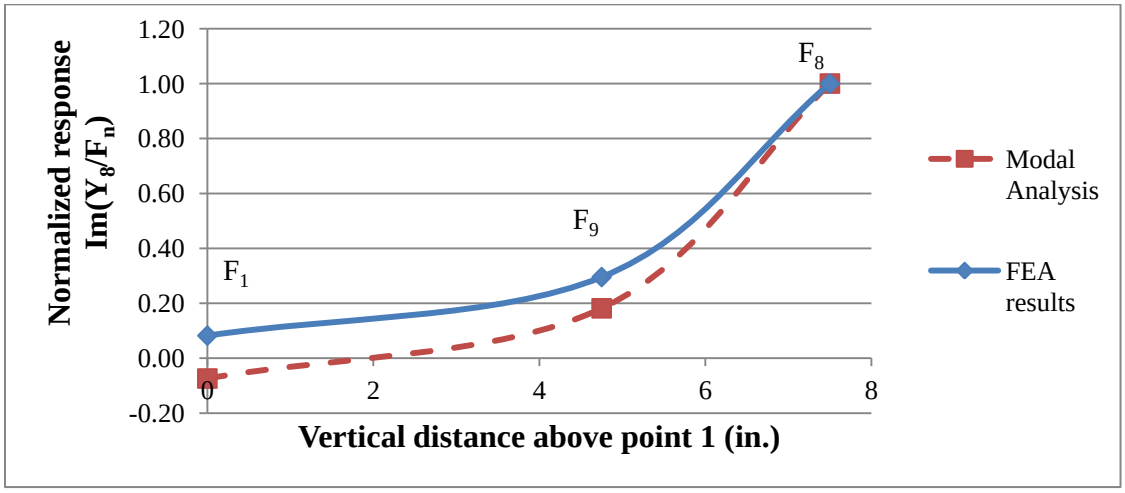

FIGURE 13 : Normalized mode shape comparison of 1B and 1F for the shifter handle in the y-direction

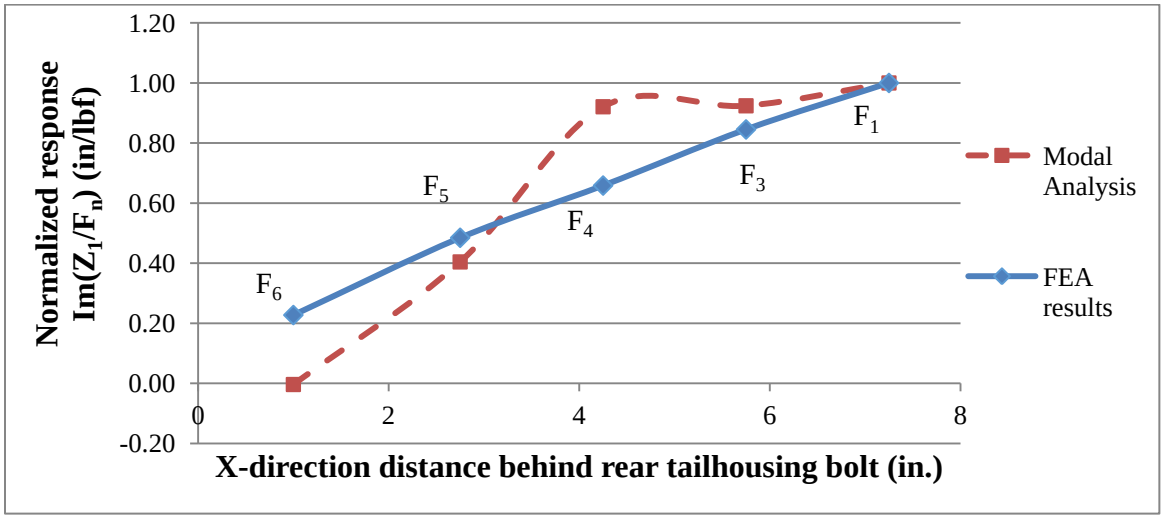

FIGURE 14 : Normalized mode shape comparison of 2B and 2F for the setback brackets in the z-direction

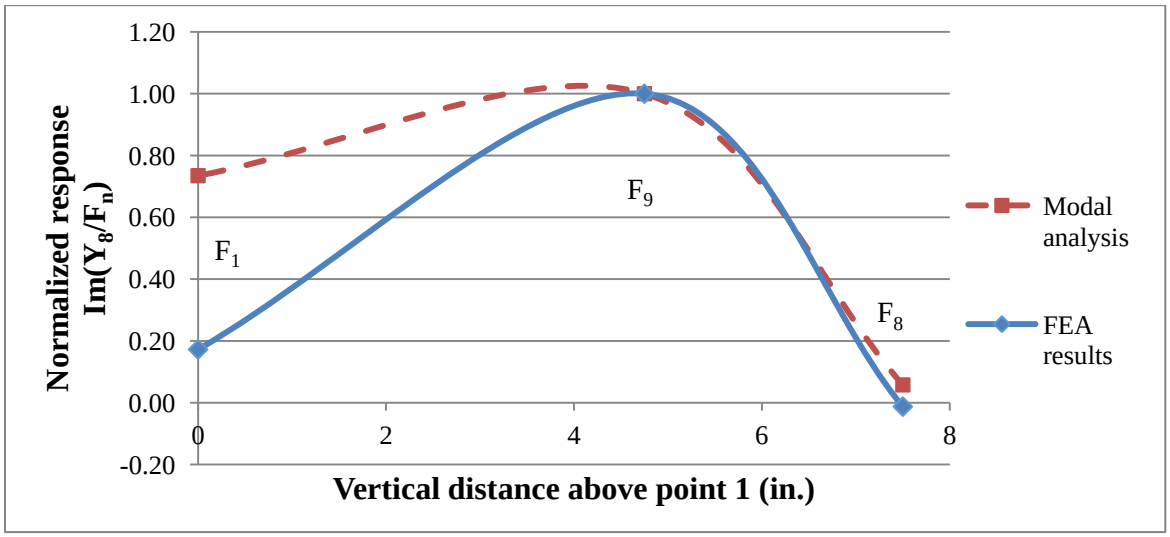

FIGURE 15 : Normalized mode shape comparison of 2B and 2F or the shifter handle in the x-direction

The mode shapes given by 3B and 3F are similar to that of the second mode of a cantilever. Here, the y and z-direction vibrations are more distinctive with the former more prominent in the handle (FIGURE 16) and the latter in the setback brackets

(FIGURE 27). The phase change may be seen in the y-direction response as the node is near the center of the graph (F_9) with the two ends out of phase with one other.

Each of the mode shape comparisons yield comparable results between the FEA model and modal analysis for the simplified block. Combined with the natural frequency agreement, it is determined that the FEA model is a sufficient representation of the simplified model relative to the response of the physical assembly.

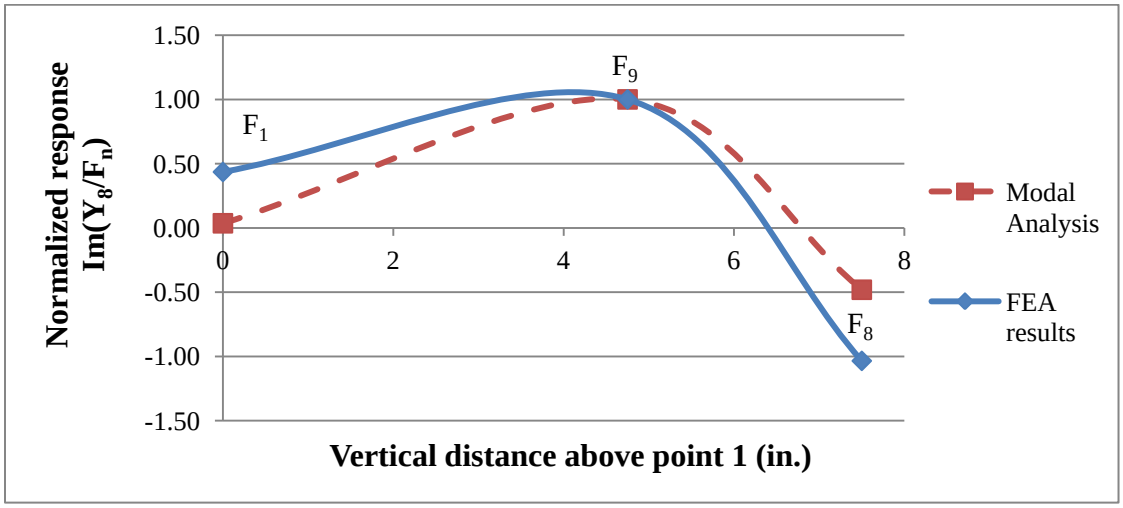

FIGURE 16 : Normalized mode shape comparison of 3B and 3F for the shifter handle in the y-direction

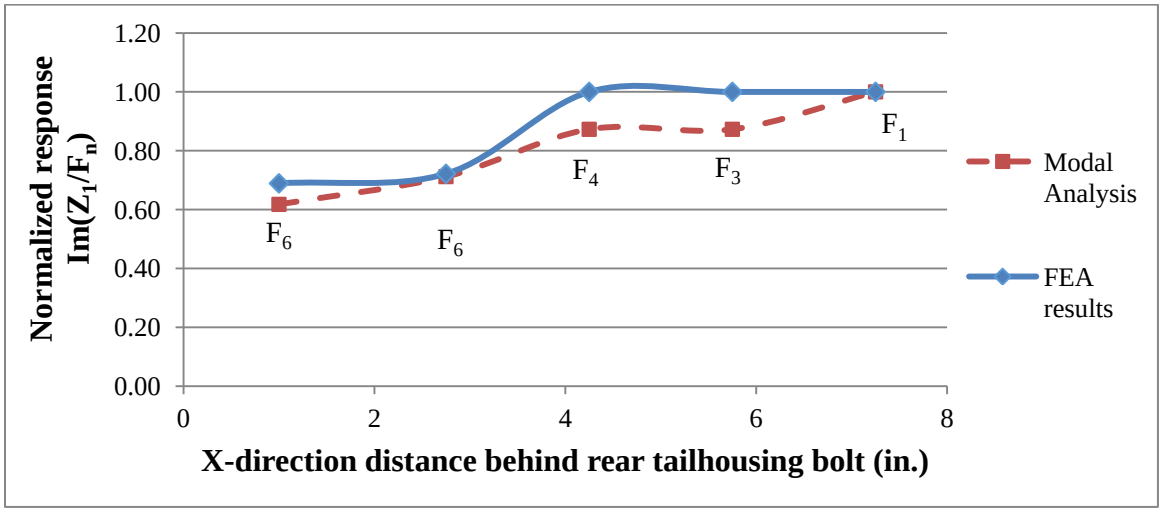

FIGURE 17 : Normalized mode shape comparison of 3B and 3F for the setback brackets in the z-direction

3.2 Comparison of Physical Simplified Model and Real World (in-car) Use

The measured FRFs completed on the simplified setup and stock car are reported in this section. First, the results of the analysis in the car are presented. Then, the comparison between the two analyses is completed.

The modes determined from modal analysis in the car are displayed according to the coordinate axes in which the vibration takes place; see TABLE 5. As before, the modes under 50 Hz are not included in the table. The modes in the table are designated with a "C" to denote the car measurements. It is observed that connecting the shifter assembly to the other components in the car resulted in a greater number of modes than were found in the simplified model.

The mode shapes are now compared between the three frequencies obtained in the modal analysis of the block setup to that of the car. The modes of the two analyses are organized according to their shapes and are compared in TABLE 6. As displayed in the table, the three shapes observed in the simplified analysis are evident in the car. Modes2B and 3B were consistent in both shape and the frequency at which they occurred. However, mode 1B – the handle vibrating the y-direction – saw a decrease

TABLE 5 : Natural frequencies determined from frequency response of car system

Mode	Frequency (Hz)		
	X	Y	Z
1C		110.6	111.9
2C		118.3	
3C	133.2		135.8
4C			144.2
5C	169.0	169.0	
6C	271.2	272.8	273.5

greater than 16% when compared to the response in the car.

The mode shapes for the modes listed in TABLE 6 are illustrated in Figures 18-23. Other mode shapes from the car can be found in Appendix V.

TABLE 6 : Comparison of similar modes from modal analysis for the simplified model and the car

Simplified Model (Block)		Car System		% Difference
Mode	Frequency (Hz)	Mode	Frequency (Hz)	
1B	141.5	2C	118.3	-16.4%
2B	146.4	3C	134.5	-8.1%
3B	271.9	6C	272.5	0.2%

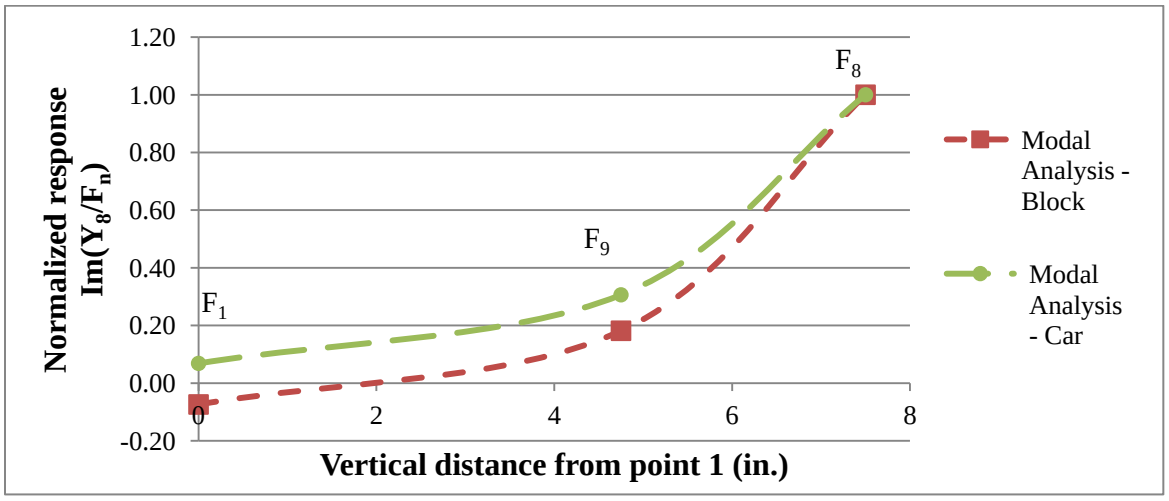

FIGURE 18 : Normalized mode shape comparison of 1B and 2C for the shifter handle in the y-direction

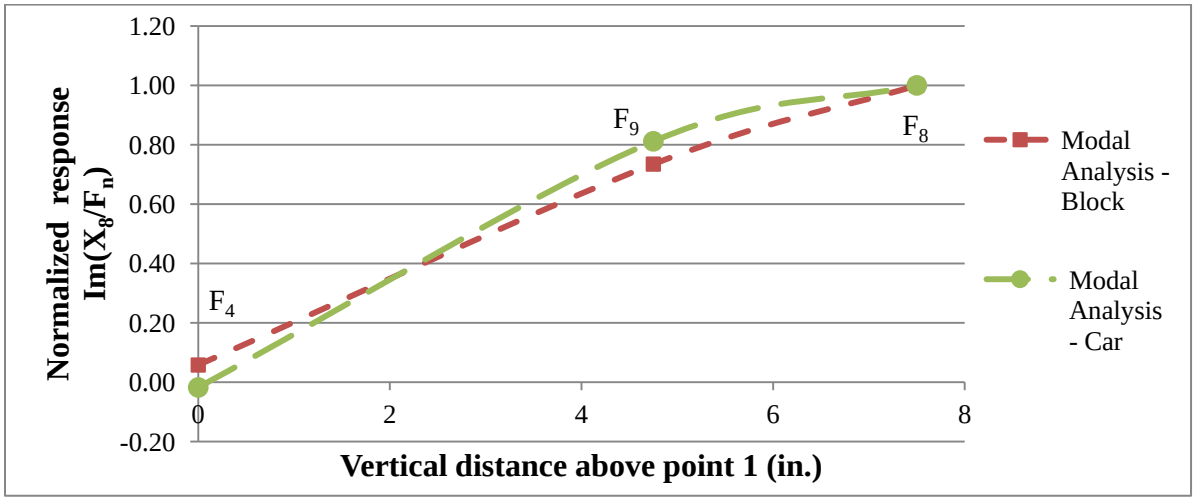

FIGURE 19 : Normalized mode shape comparison of 2B and 3C for the shifter handle in the x-direction

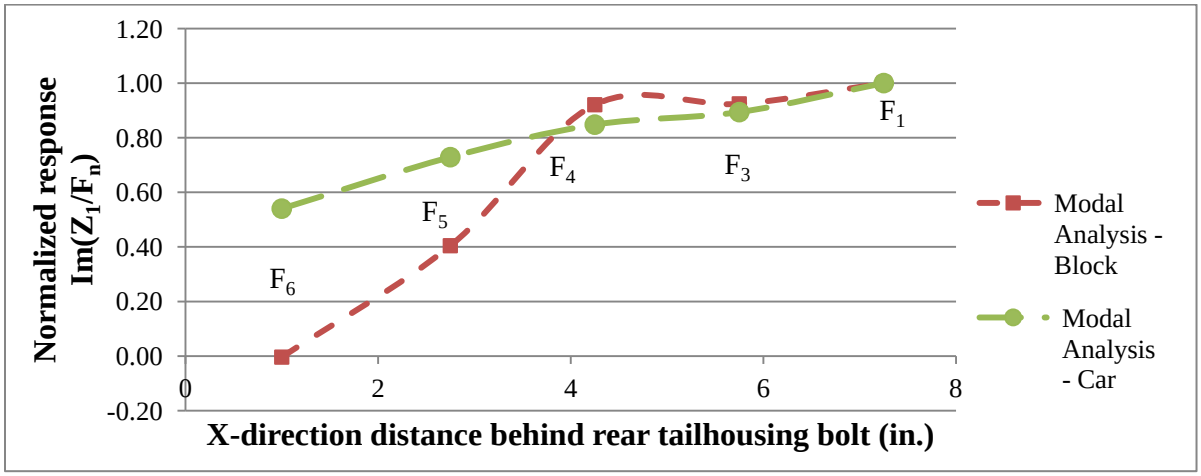

FIGURE 20 : Normalized mode shape comparison of 2B and 3C for the setback brackets in the z-direction

The mode shape difference in the z-direction in FIGURE 20 is attributed to the addition of the tail housing. The, effective cantilever length is increased in the car with a pivot at the front of the transmission. This longer cantilever yields the offset in the

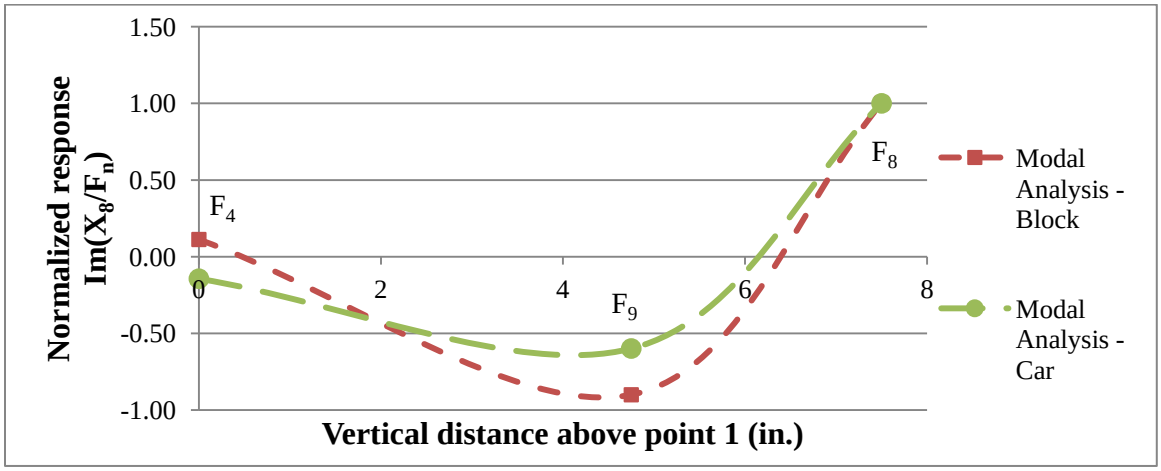

FIGURE 21 : Normalized mode shape comparison of 3B and 6C for the shifter handle in the x-direction

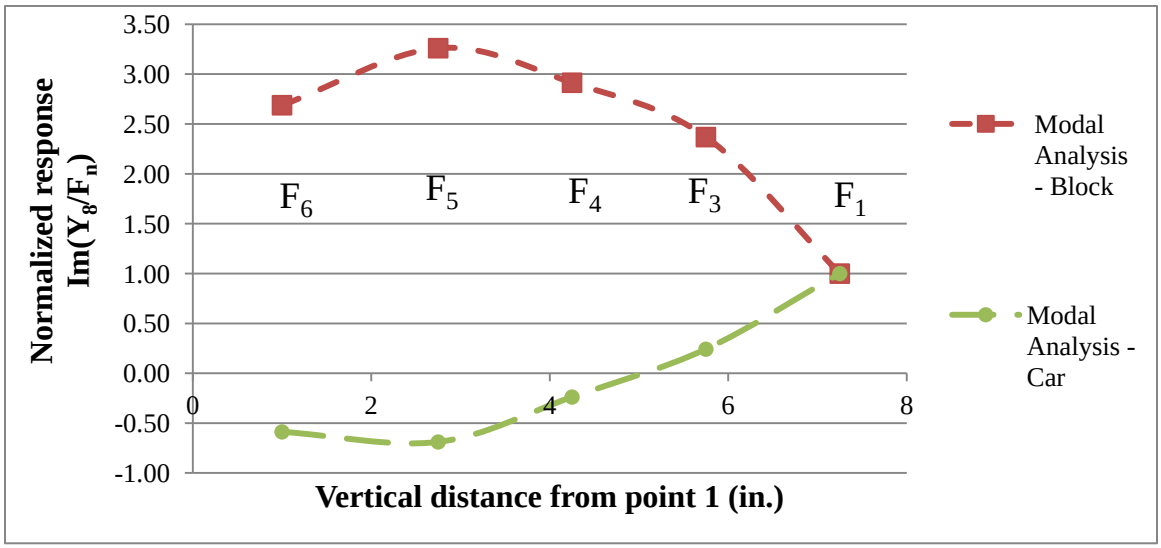

FIGURE 22 : Normalized mode shape comparison of 3B and 6C for the setback brackets in the y-direction

measurements taken closer to the setback bracket mount at the tail housing.

Again, the setback brackets and the shifter handle are separated for the measurements in the y-direction. The mode shapes agree between the simplified model and the car analyses.

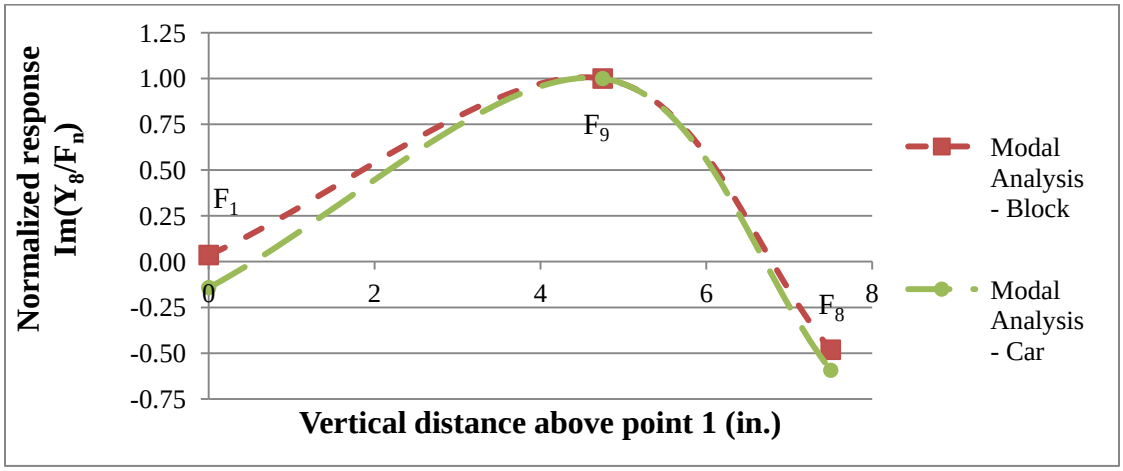

FIGURE 23 : Normalized mode shape comparison of 3B and 6C for the shifter handle in the y-direction

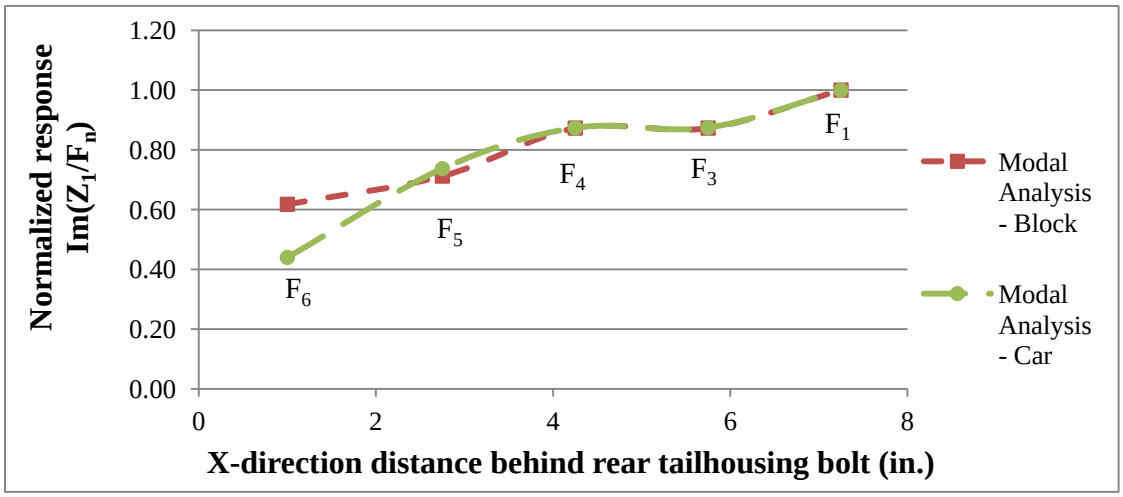

FIGURE 24 : Normalized mode shape comparison of 3B and 6C for the shifter handle in the z-direction

For further comparison, Figures 25, 26, and 27 compare the real and imaginary parts of the FRFS from the two tests in the x, y, and z directions, respectively. The x-direction provides the greatest correlation between the two setups in terms of frequencies and magnitudes.

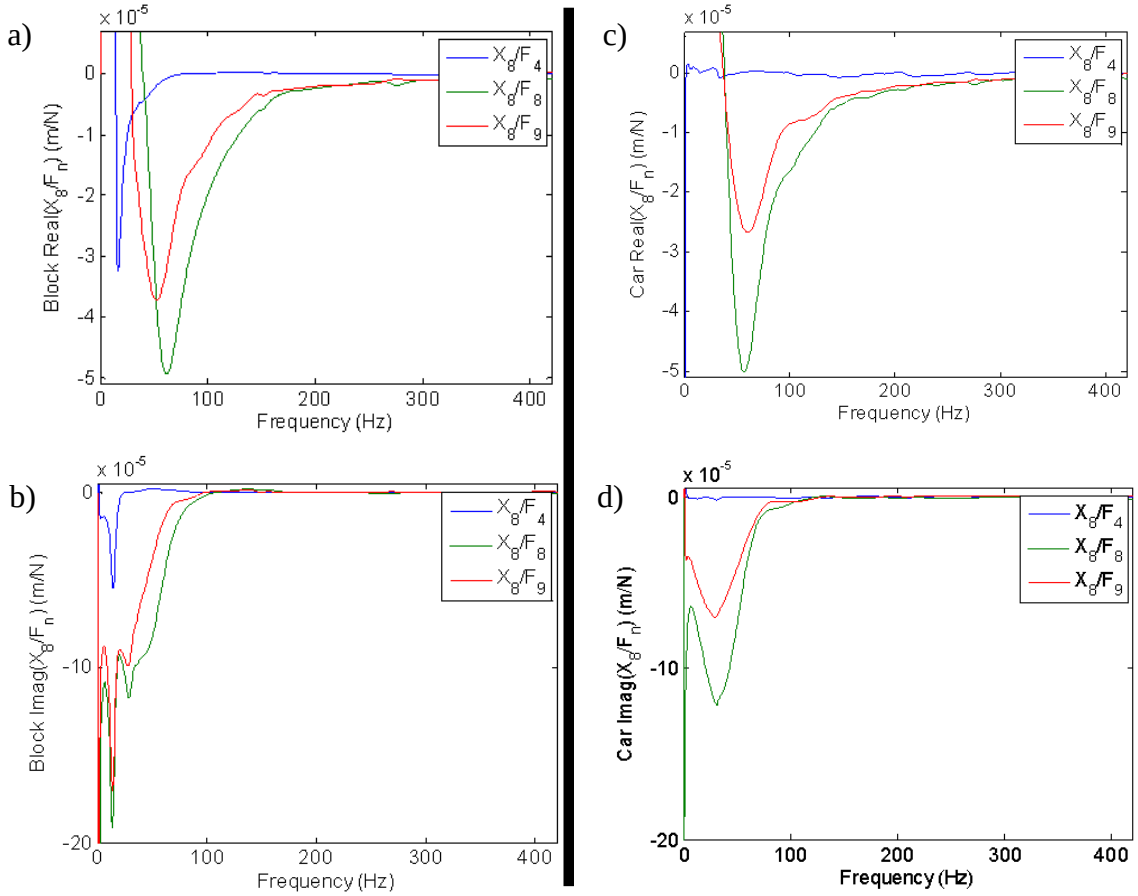

FIGURE 25 : X-direction overview comparison of simplified (left) and stock car (right) measurements

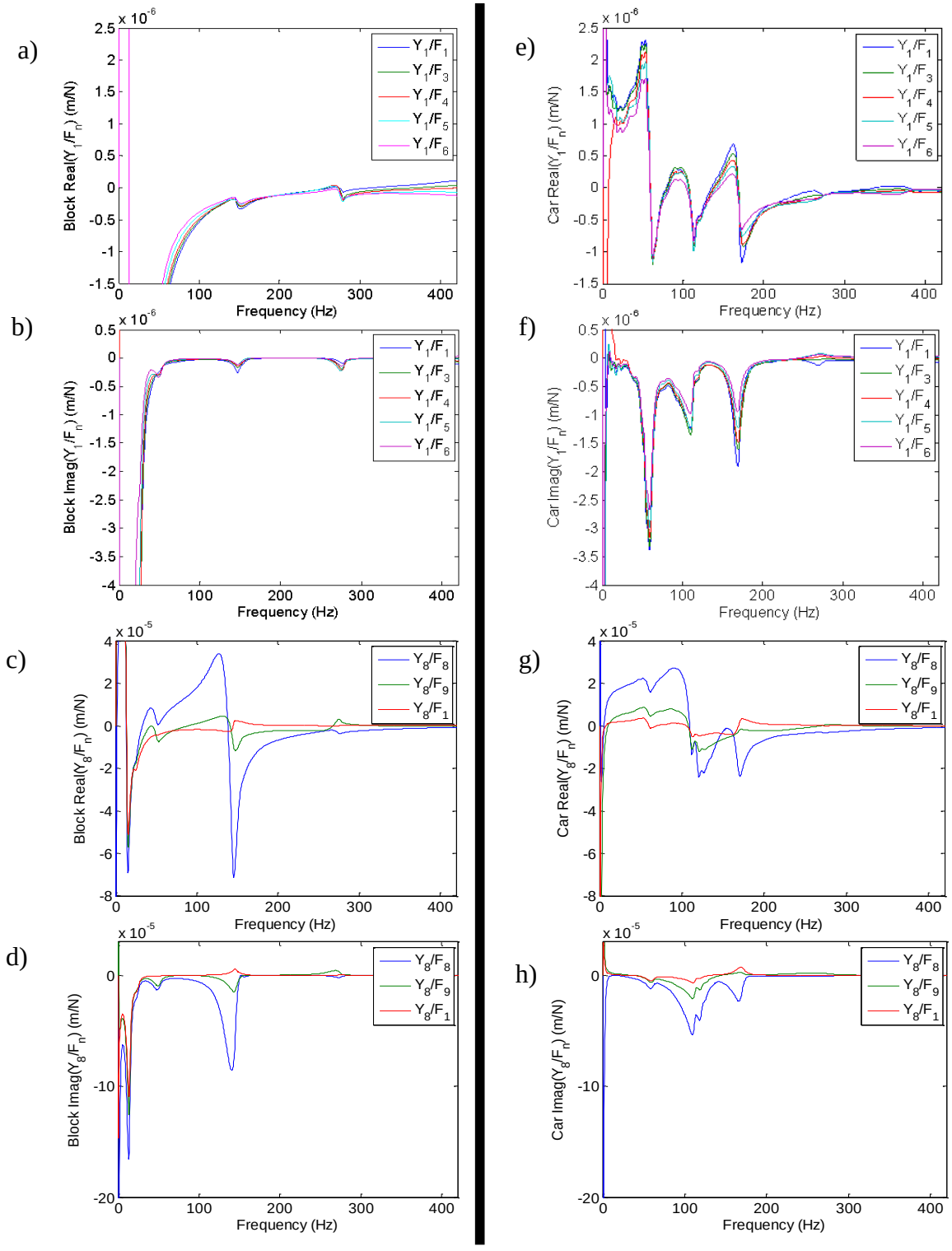

FIGURE 26 : Y-direction overview comparison of simplified (left) and stock car (right) measurements

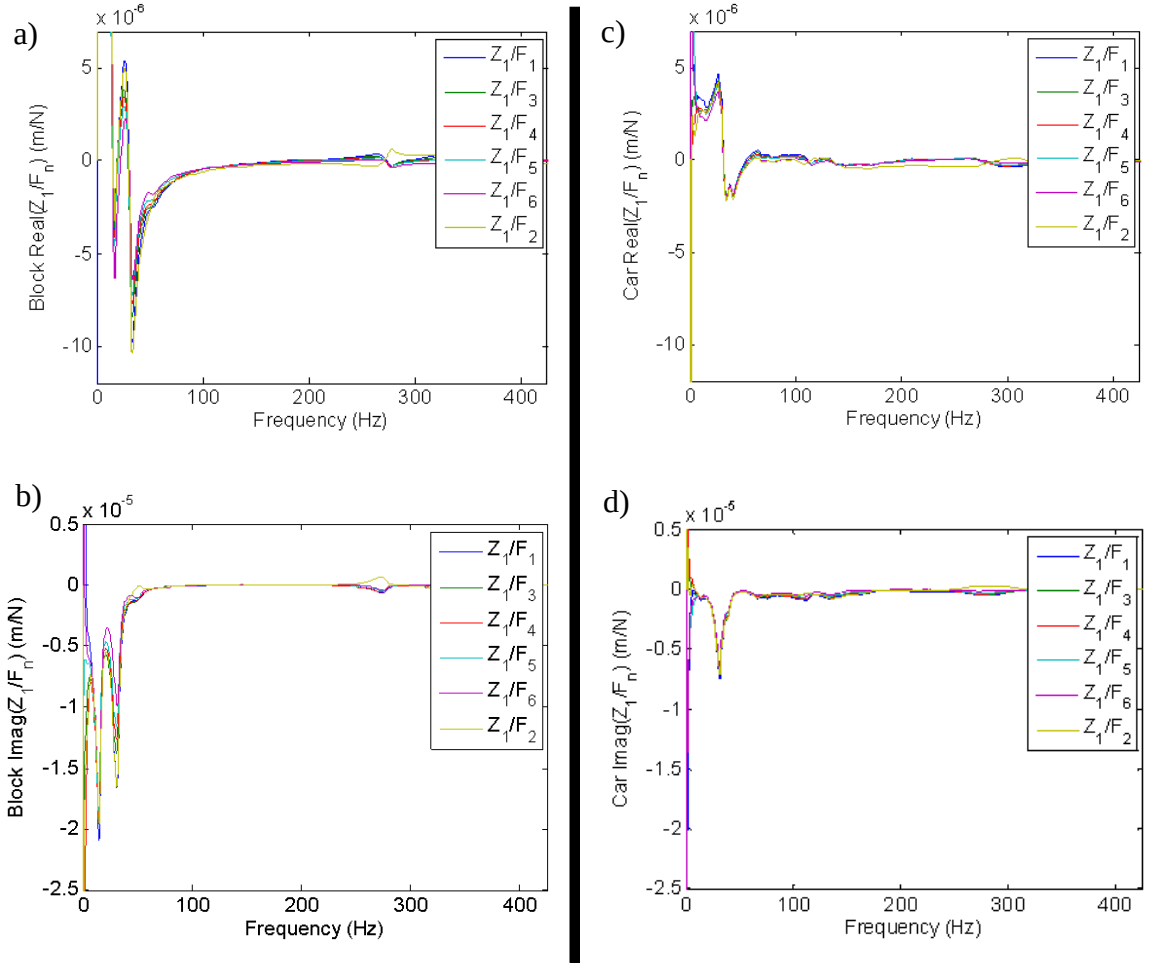

FIGURE 27 : Z-direction overview comparison of simplified (left) and stock car (right) measurements

CHAPTER 4: CONCLUSION

4.1 Analysis of Results

The FEA model is considered to be sufficient when compared to the modal analysis results on the physical representation of the simplified model. All three mode shapes obtained from the FEA were apparent in the frequency response of the physical model. The natural frequencies of two modes were within 5.0% of the FEA results, while one result differed by 20.6%.

While the modal analysis of the simplified model does not provide an exact correlation to the data extracted from the system installed in the vehicle, similarities between the two may be drawn. To begin, all three obtained from the simplified model are evident in the stock car as well, although one mode's shape changed slightly. The differences in frequencies at which these three modes occur are 0.2% to 16.4% when comparing the simplified model to stock car measurements. Modes in the car generally increase in magnitude over their counterparts in the simplified model as a result of the inherent flexibility in the drivetrain.

Furthermore, three modes are present in the car that are not found in the simplified model. These modes are a result of other components in the drivetrain, such as the shifter linkages, tailhousing, and driveshaft, which add natural frequencies to the system. As these frequencies are close in relation to those found in the simplified model, they would likely have an impact on the results of the sensitivity study matrix.

Additionally, with these components having similar frequencies, the largest of the three comparable modes had an additional node in the y-direction in the car, but did not change in the other two directions.

4.2 Future Work

As the simplified model and in-car modal analysis results did not agree perfectly, there is room to improve the model before the sensitivity study. The results showed that proceeding with evaluating the sensitivity of the system via changes in either the setback brackets or the shifter handles may currently be skewed by modes from other drivetrain components. The planned matrix for the study is shown in TABLE 7.

TABLE 7 : Proposed cases for sensitivity study

Case	Setback Brackets	Shifter Handle Material
1	26”	7075 Aluminum
2	26”	1018 Mild Steel
3	24”	7075 Aluminum
4	24”	1018 Mild Steel

The modes that were evident from the car analysis may be used to improve the FEA model. This can be achieved by adding spring-mass systems at the pinned constraints to simulate the modes from the drivetrain components. The acceptable model should be determined through the modes obtained from the car. This is important as the natural frequencies observed from the drivetrain are near those from the shifter assembly. The possibility exists that any changes in the shifter assembly could actually align with an existing mode. If that were the case, it could either increase the magnitude of that vibration or reduce it similar to the effect of a mass damper. Once an acceptable FEA model is obtained, it may be used to evaluate the matrix proposed in this paper as well as other related studies.

REFERENCES

Ewins, D. J. (1995). *Modal testing : theory and practice* (Rev. with new notation ed.). Taunton, Somerset, England New York: Research Studies Press ;Wiley.

Schmitz, T. L., & Smith, K. S. (2012). *Mechanical vibrations : modeling and measurement*. New York, NY: Springer Science+Business Media, LLC.

APPENDIX A : MEASUREMENT AND EXPERIMENT EQUIPMENT

The following table lists serial and model numbers for the impact analysis equipment.

TABLE 8 : Model and serial numbers for impact analysis equipment

Data Acquisition Board	Model: DT9837B
Piezoelectric Accelerometer	Model: 352A21 SN: 128850
Impact Hammer	Model: 086C04 SN:29958

APPENDIX B : PART DRAWING

The engineering drawing for the test block used in the modal analysis performed on the physical representation of the simplified model is displayed on the following page. The image has been scaled down in order to be located in this document.

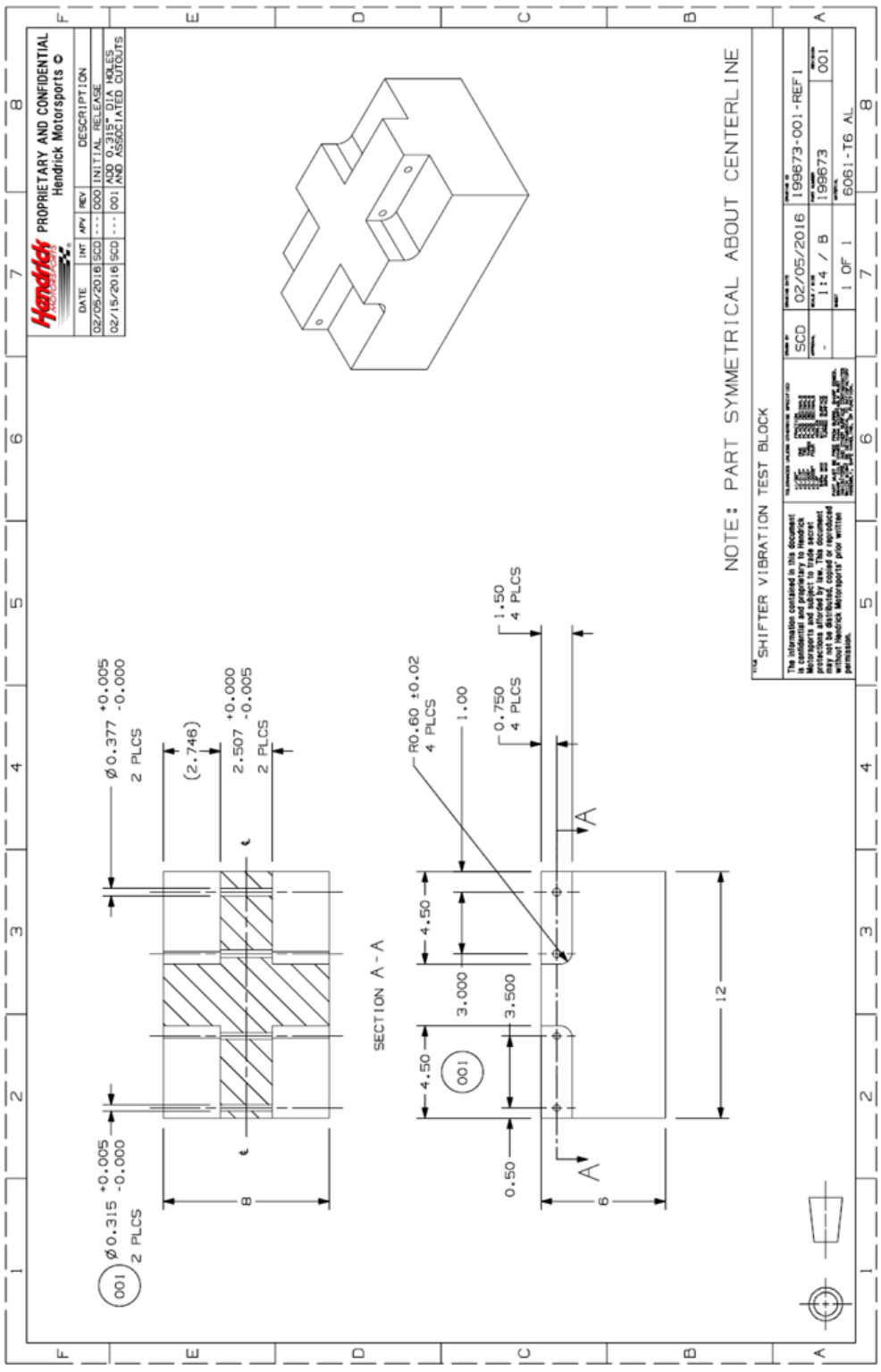

FIGURE 28 : Engineering drawing of the block used in modal testing of the simplified model

APPENDIX C : ADDITIONAL DIAGRAMS OF FEA RESULTS

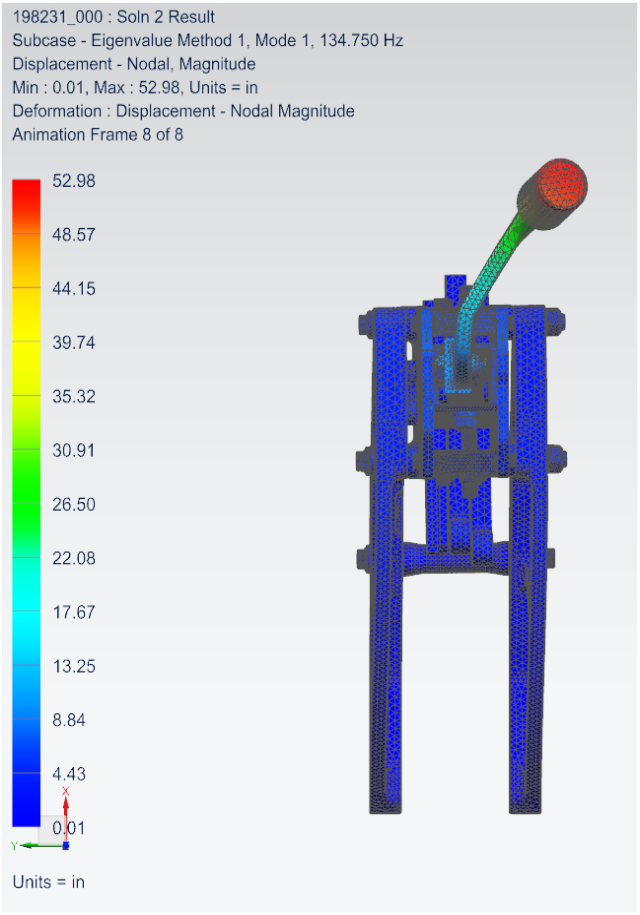

FIGURE 29 : Mode 1F looking at the xy-plane from the +z direction

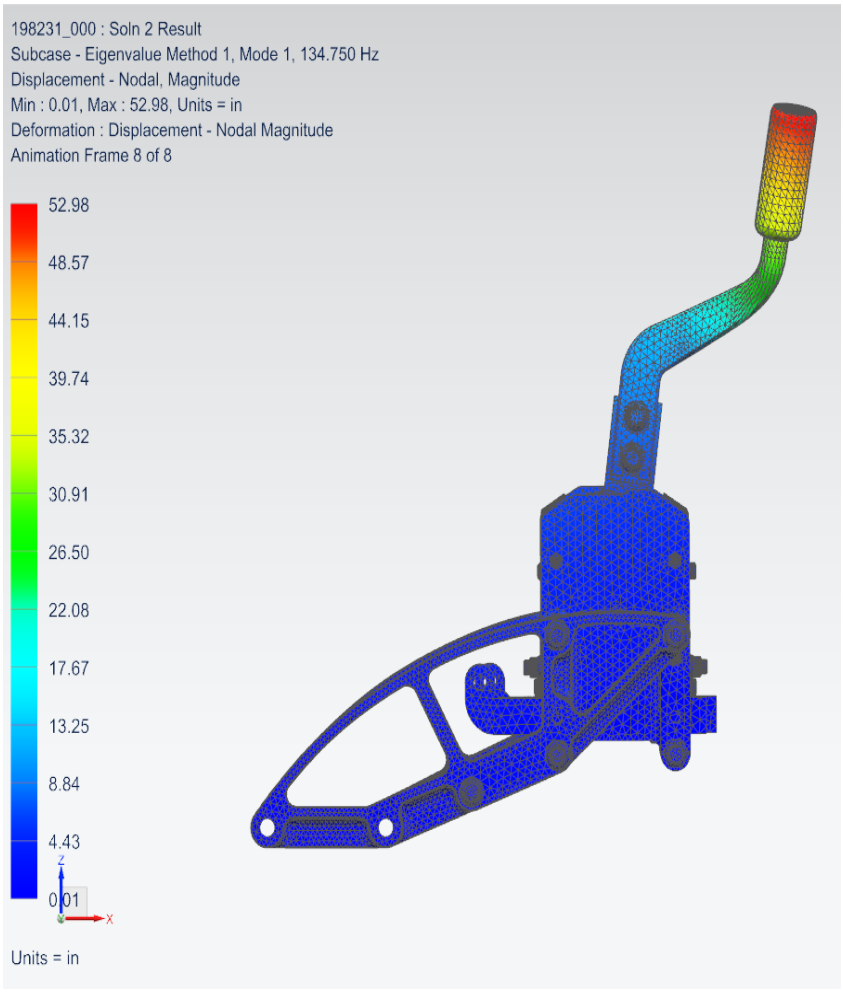

FIGURE 30 : Mode 1F looking at the xz-plane from the –y direction

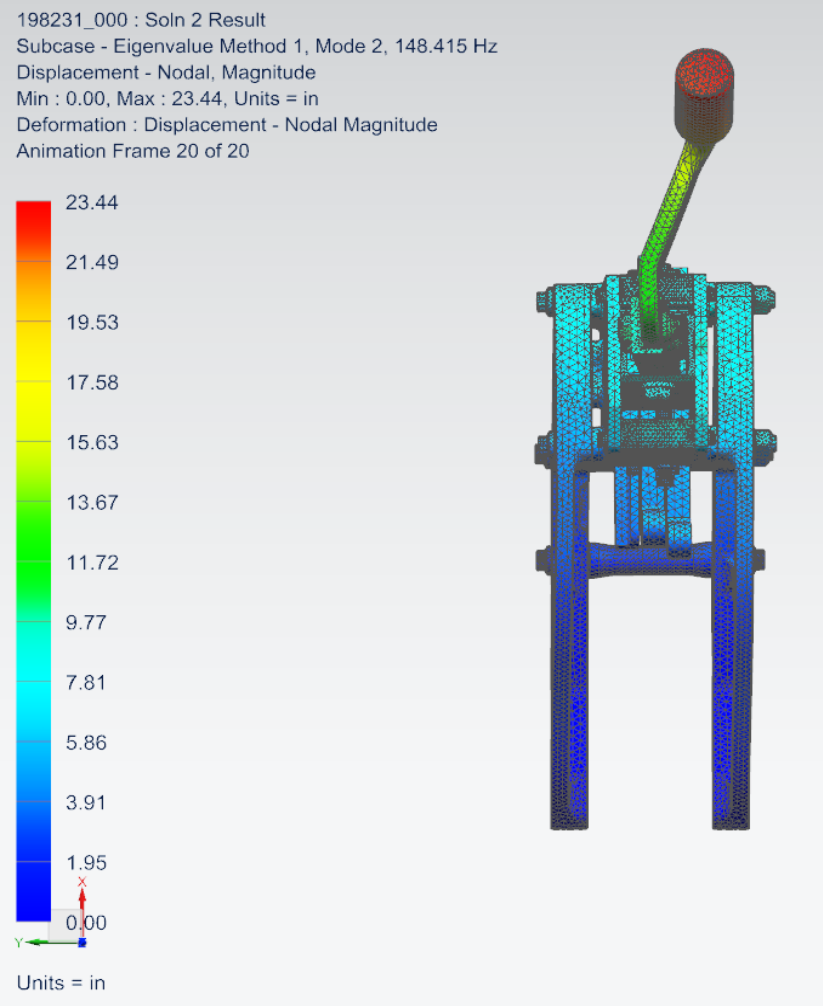

FIGURE 31 : Mode 2F looking at the xy-plane from the +z direction

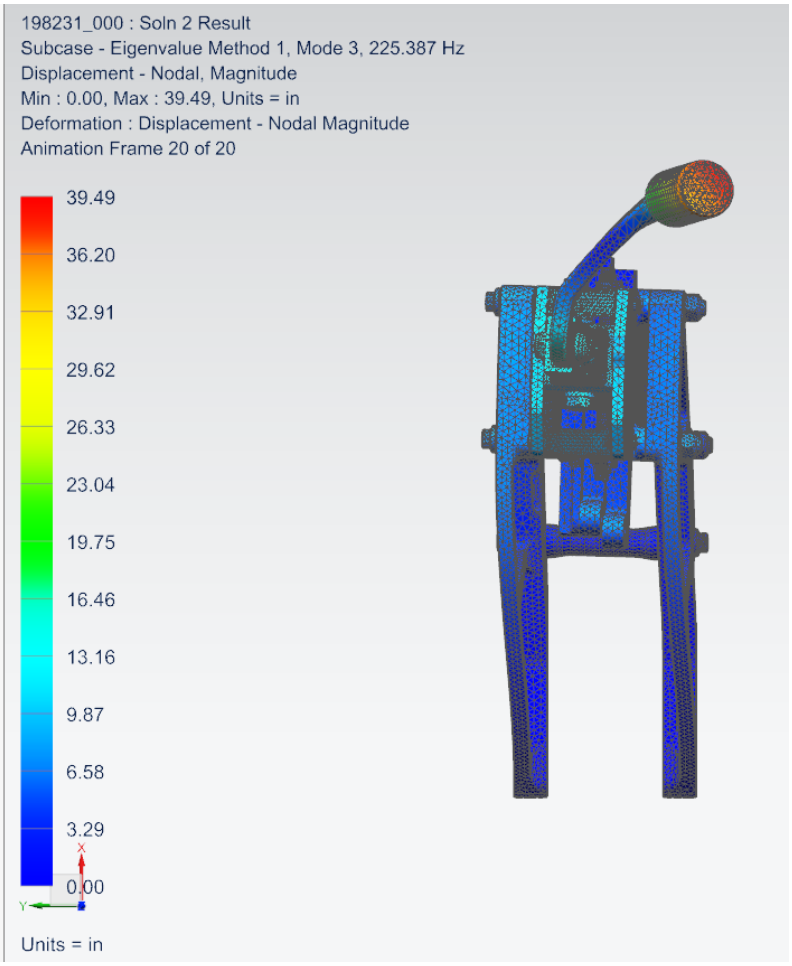

FIGURE 32 : Mode 3F looking at the xy-plane from the +z direction

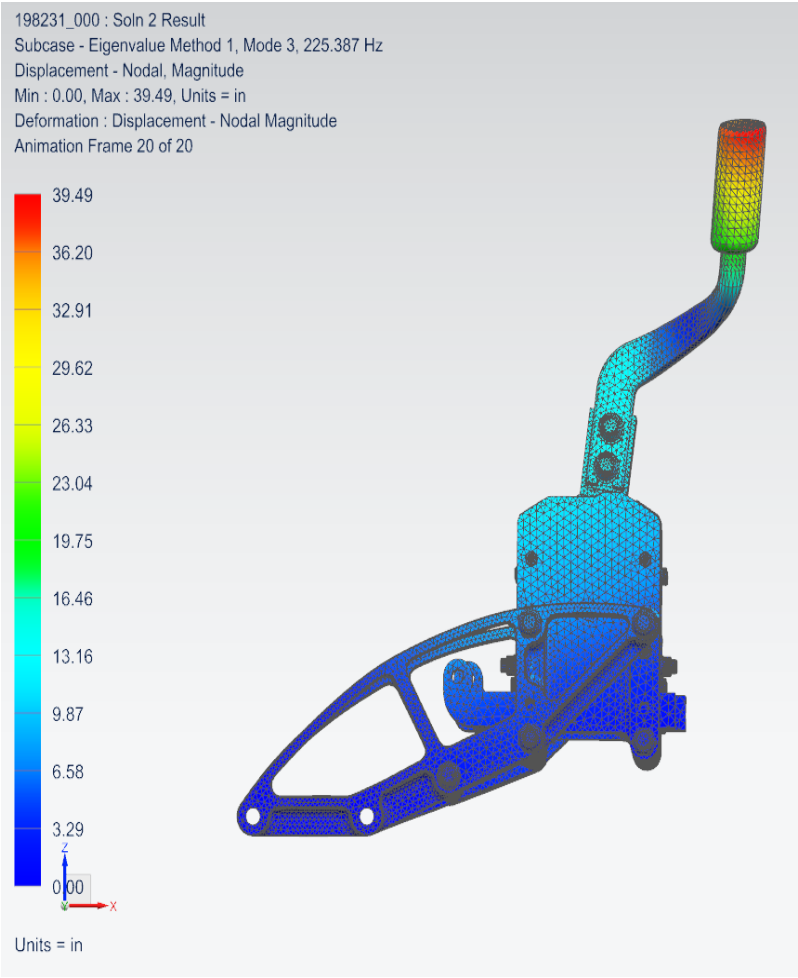

FIGURE 33 : Mode 3F looking at the xz-plane from the –y direction

APPENDIX D : IMAGES OF MODAL TESTING

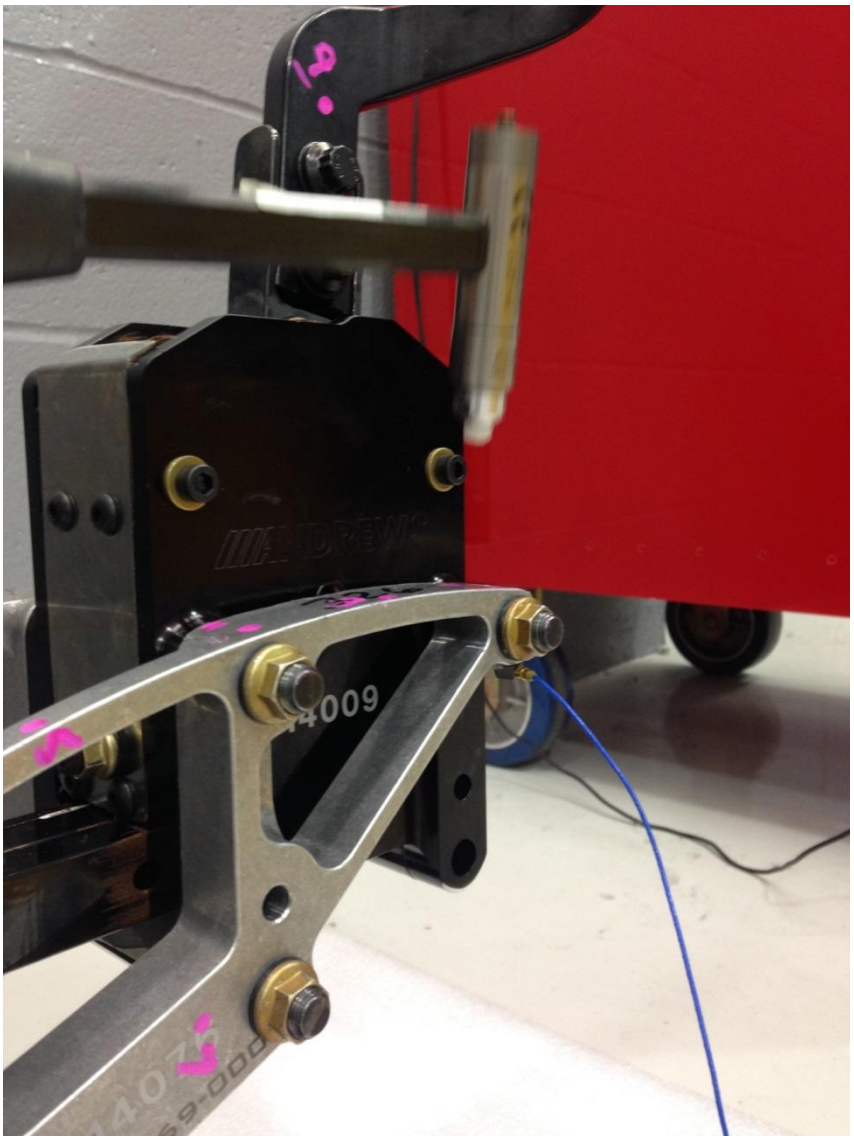

FIGURE 34 : Physical modal testing (Z_1/F_1) on the simplified model

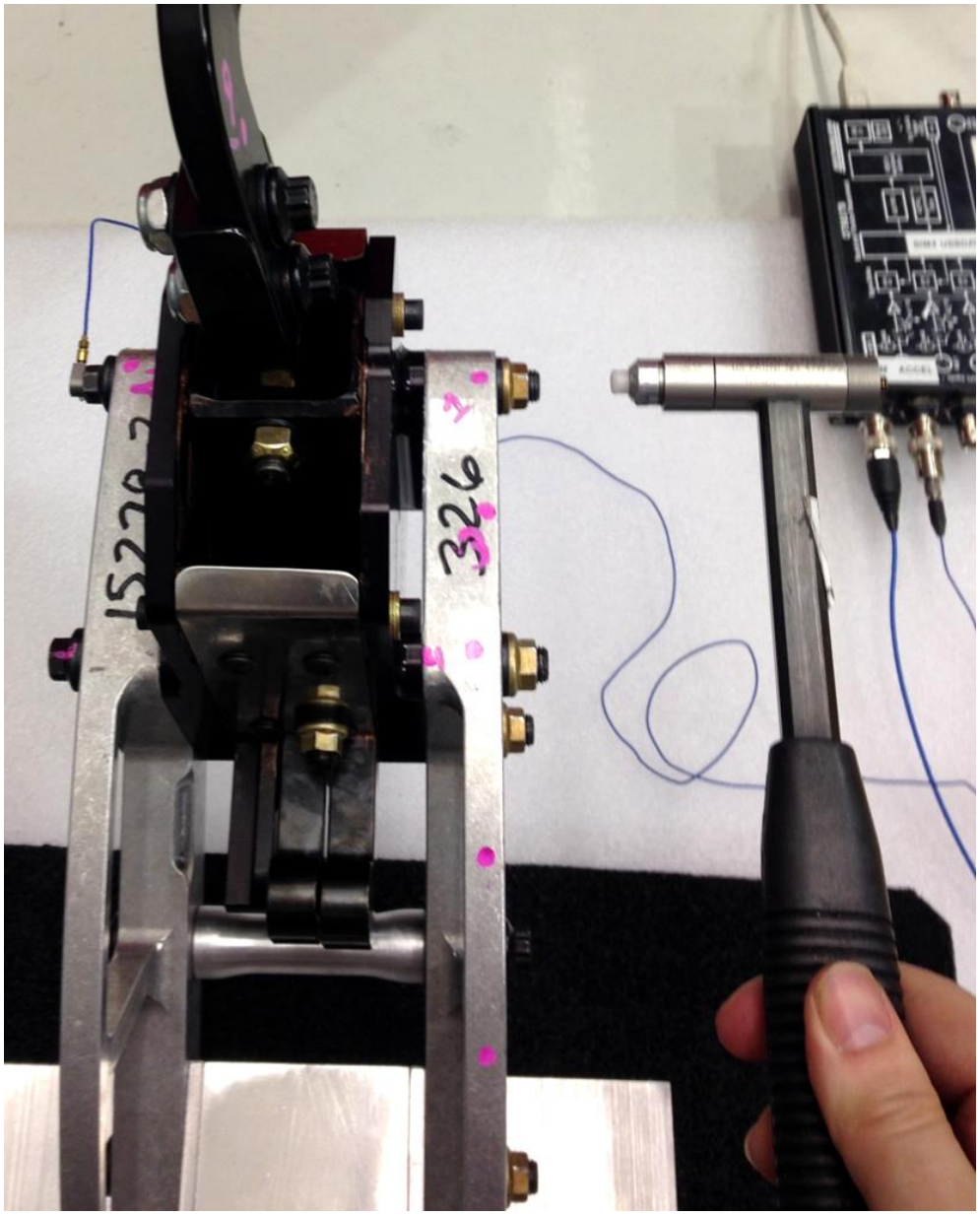

FIGURE 35 : Physical modal testing (Y_1/F_1) on the simplified model

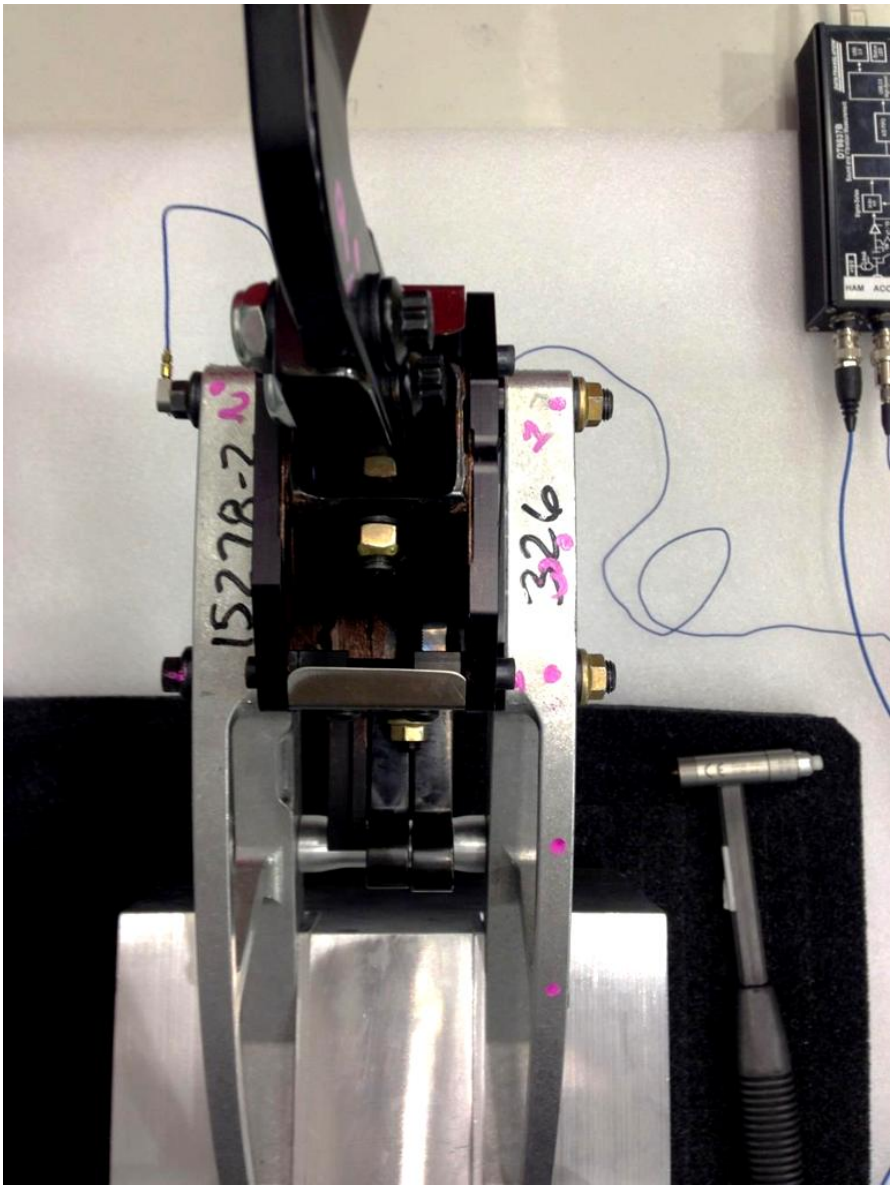

FIGURE 36 : Preparation for modal testing (Y_1/F_n) on the simplified model

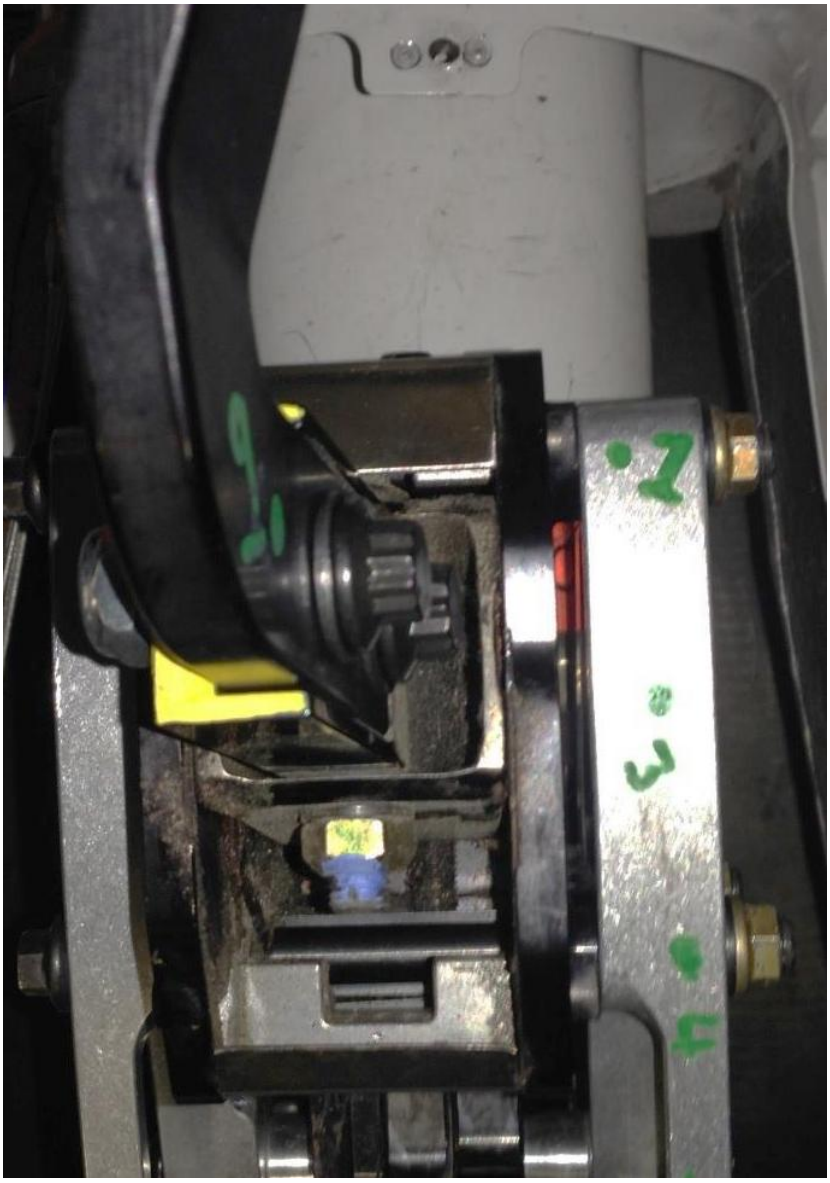

FIGURE 37 : Preparation for modal testing (Y_1/F_n) in the car

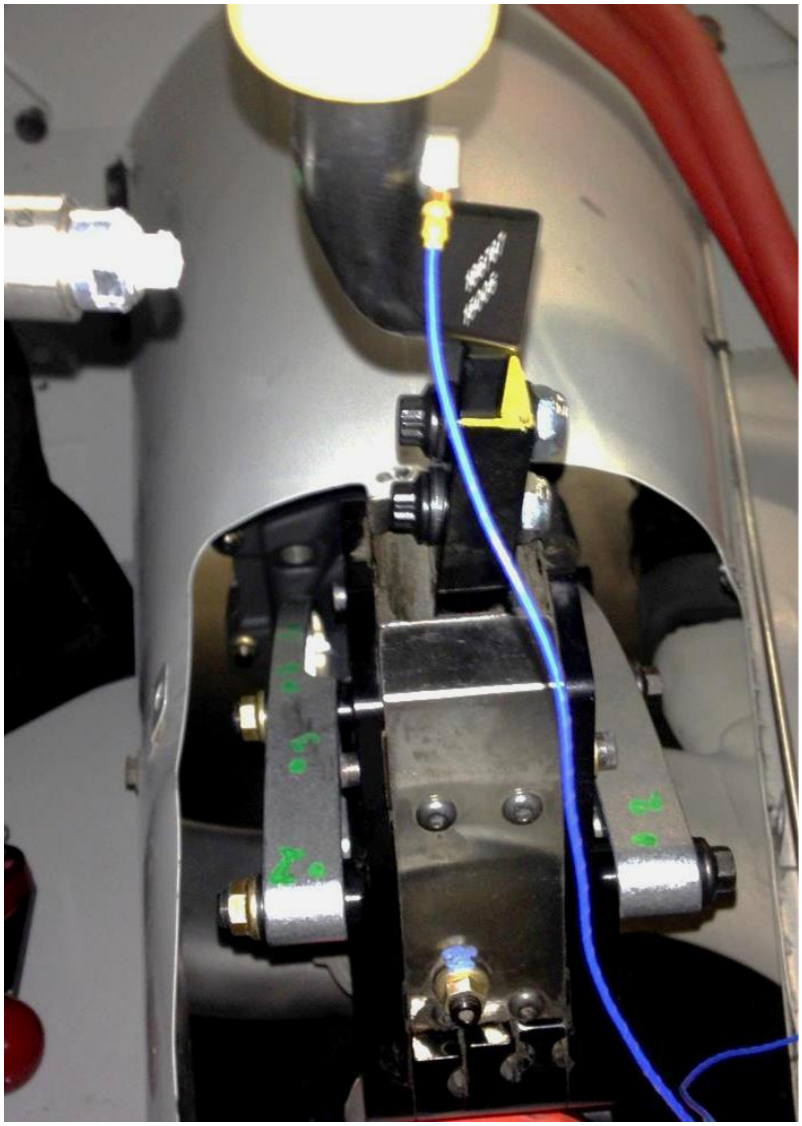

FIGURE 38 : Physical in-car modal testing (Y_8/F_8)

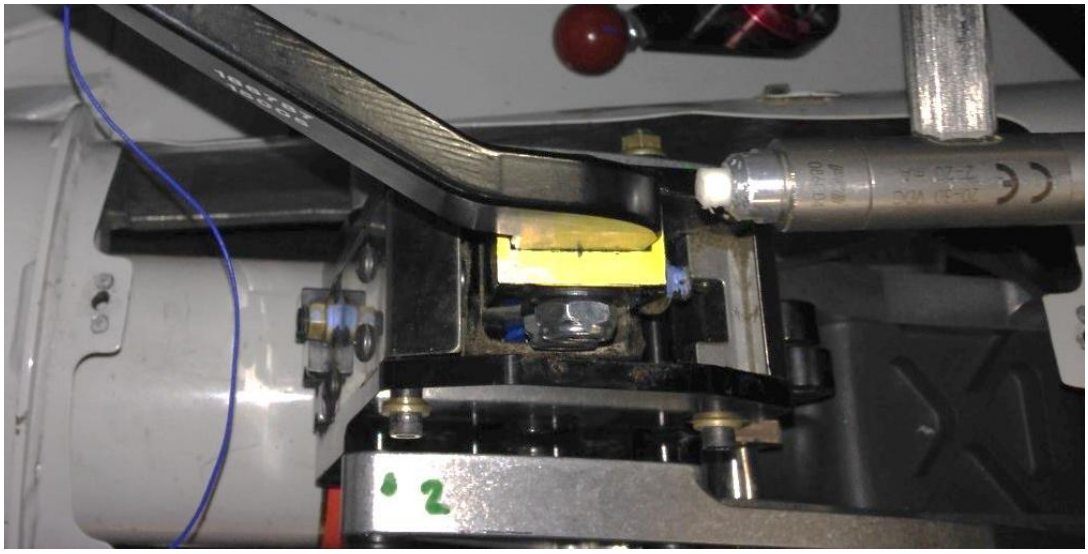

FIGURE 39 : Physical in-car modal testing (X_8/F_9)

APPENDIX E : ADDITIONAL CAR MODE SHAPES

The first mode that appeared in the car that was not visible in the simplified model was 1C at an average of 111.2 Hz. It appeared in both the y and z-directions. The y-shape is nearly two orders of magnitude larger in the handle than in the setback brackets.

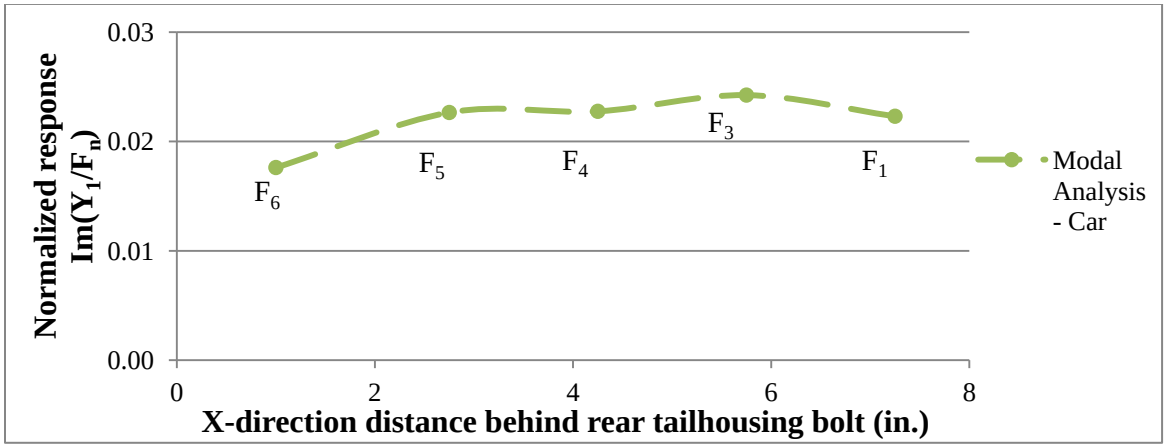

FIGURE 40 : Normalized mode shape of 1C for the setback brackets in the y-direction

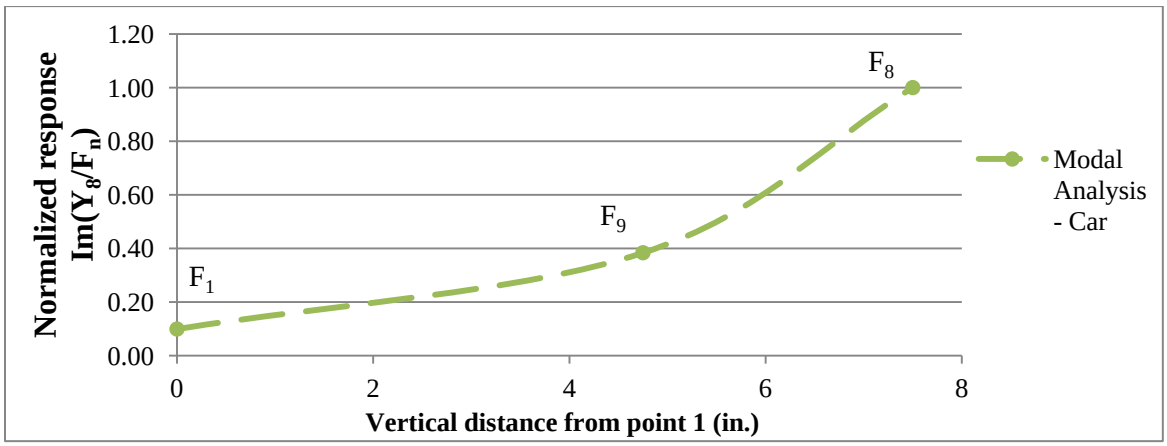

FIGURE 41 : Normalized mode shape of 1C for the shifter handle in the y-direction

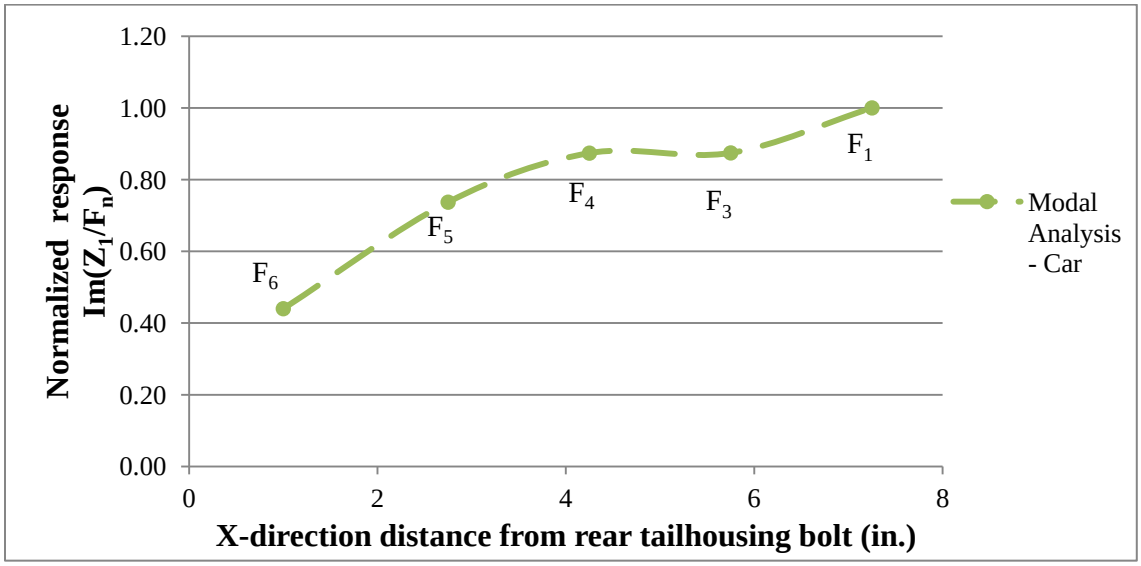

FIGURE 42 : Normalized mode shape of 1C for the setback brackets in the z-direction

The second mode that was only evident in the car was a z-directional mode, 4C, at 144.2 Hz. The mode shape for 4C is displayed in FIGURE 43.

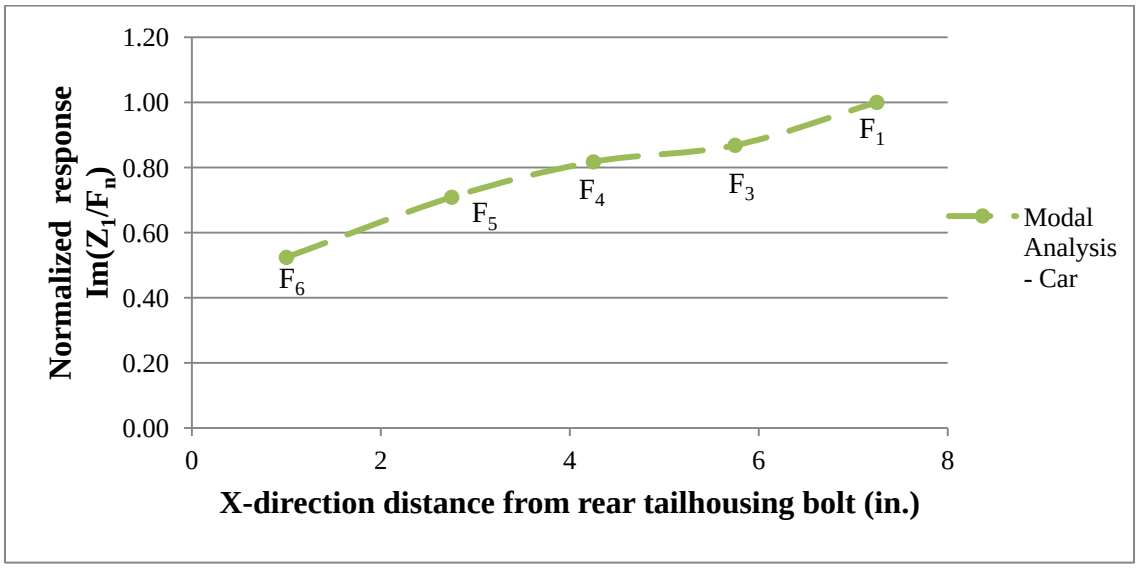

FIGURE 43 : Normalized mode shape of 4C for the setback brackets in the z-direction

Mode 5C was the third mode that was different between the simplified model and the car. It appeared in the x and y-directions at 169.0 Hz. This is evidence of a twisting mode mainly in the handle itself as there was an order of magnitude less movement in the shifter brackets as compared to the shifter handle.

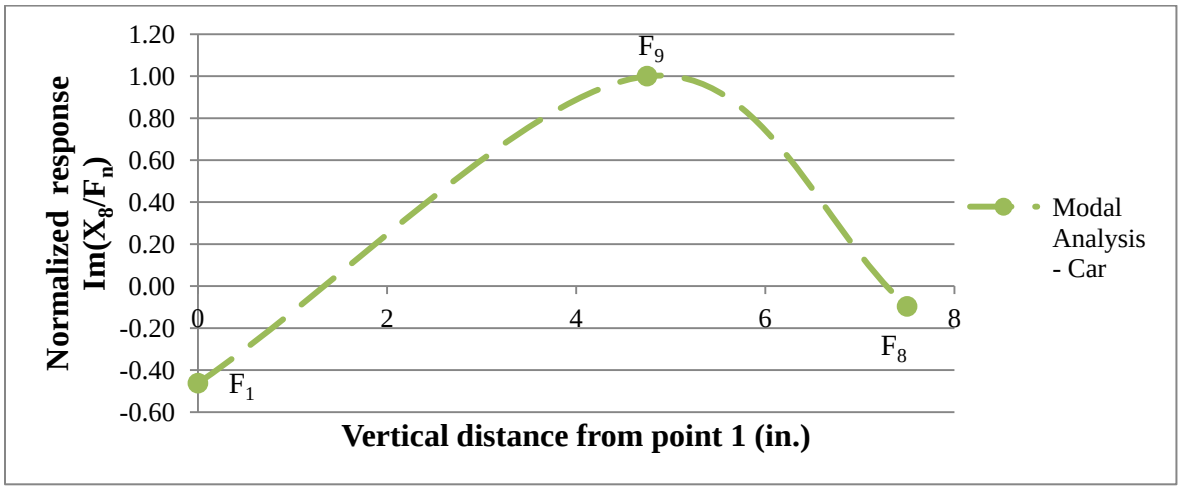

FIGURE 44 : Normalized mode shape of 5C for the shifter handle in the x-direction

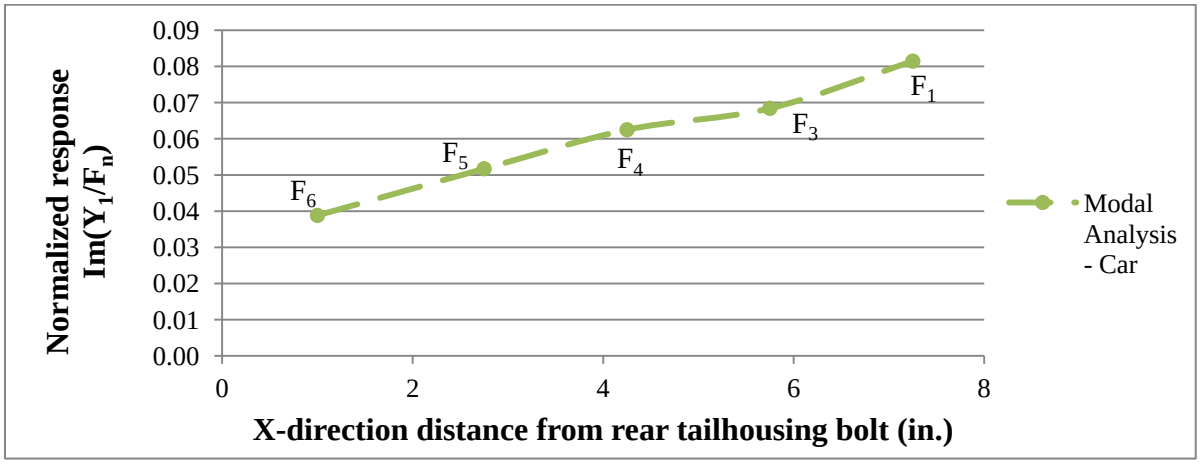

FIGURE 45 : Normalized mode shape of 5C for the setback brackets in the y-direction

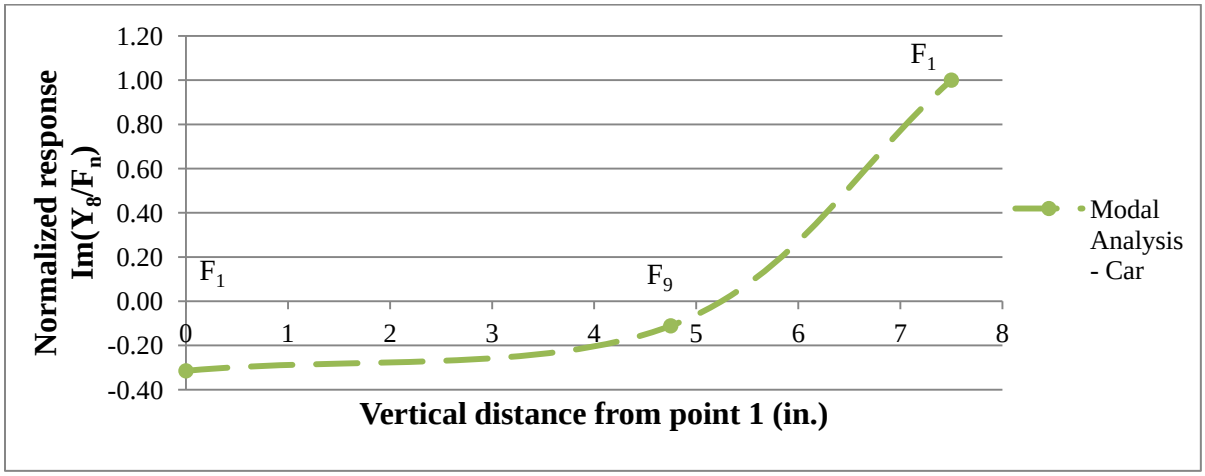

FIGURE 46 : Normalized mode shape of 5C for the shifter handle in the y-direction